Cancer Res 1988;48:793–7; 194. *Anticancer Res* 1995;15:1297–302; 195. *Br J Cancer* 2003;89:185–91; 196. *Tumori* 1989;75:423–8; 197. *Eur J Cancer* 1991;27:673; 198. *Clin Cancer Res* 2003;9:1161–70; 199. *Cancer Res* 2001;61:3986–97; 200. *Mol Cancer Ther* 2002;1:707–17; 201. *Anticancer Res* 2000;20:407–16; 202. *J Biol Chem* 2003;278:23432–40; 203. *Nat Med* 1999;5:662–8; 204. *Oncogene* 2001;20:4995–5004; 205. *Mol Pharmacol* 2002;62:689–97; 206. *Biochem Pharmacol* 2000;59:337–45; 207. *Proc Natl Acad Sci USA* 1991;88:10591–5; 208. *Cancer Res* 1997;57:2721–31; 209. *Mutat Res* 1993;303:113–20; 210. *Anticancer Drugs* 2001;12:829–34; 211. *Di Yi Jun Yi Da Xue Xue Bao* 2002;22:124–6; 212. *Br J Cancer* 1991;63:237–41; 213. *Clin Cancer Res* 1999;5:2588–95; 214. *Cancer* 1994;74:2546–54; 215. *Anticancer Res* 1996;16:1963–70; 216. *Int J Cancer* 1997;73:544–50; 217. *Br J Cancer* 2003;88:624–9; 218. *Oncogene* 2001;20:859–68; 219. *Oncogene* 2000;19:4159–69; 220. *Cancer Sci* 2003;94:467–72; 221. *Cancer Res* 1999;59:811–5; 222. *Nat Med* 1999;5:412–7. 223. *Cancer Res* 1994;54:2287–91; 224. *J Clin Endocrinol Metab* 1998;83:2516–22; 225. *Mol Carcinog* 1995;14:275–85; 226. *Oncogene* 1999;18:477–85; 227. *Cell* 1993;74:957–67; 228. *J Clin Invest* 1999;104:263–9; 229. *Br J Cancer* 1998;77:547–51; 230. *Cancer Res* 1997;57:4285–300; 231. *Breast Cancer Res Treat* 2000;61:211–6; 232. *Anticancer Res* 2000;20:5069–72; 233. *Gynecol Oncol* 2003;90:238–44; 234. *Breast Cancer Res Treat* 1999;58:99–105; 235. *Jpn J Cancer Res* 1998;89:221–7; 236. *Oncogene* 1995;10:2001–6; 237. *Anticancer Res* 2002;22:107–16; 238. *Proc Natl Acad Sci USA* 2003;100:11636–41; 239. *Cancer Cell* 2003;3:403–10; 240. *Cancer Cell* 2003;3:387–402; 241. *Cancer Res* 1994;54:3253–9; 242. *World J Gastroenterol* 1998;4:421–5; 243. *Biochem Cell Biol* 2000;78:119–26; 244. *Mol Cancer Ther* 2004;3:327–34; 245. *Int J Cancer* 1996;67:608–14; 246. *Cancer Res* 1995;55:2576–82; 247. *Gynecol Oncol* 1998;70:398–403; 248. *Chemotherapy* 2002;48:189–95; 249. *Int J Cancer* 2003;106:160–6; 250. *Cancer Res* 2000;60:6052–60; 251. *J Urol* 2001;166:461–9; 252. *J Invest Dermatol* 2003;120:1081–6; 253. *Korean J Intern Med* 1999;14:42–52; 254. *Clin Cancer Res* 2000;6:718–24; 255. *Surg Today* 1997;27:676–9; 256. *Int J Oncol* 2000;16:745–9; 257. *Int J Cancer* 1999;82:860–7; 258. *Eur J Cancer* 2001;37:531–41; 259. *Cancer Chemother Pharmacol* 2002;49:504–10; 260. *Science* 2000;290:989–92; 261. *Cancer Res* 2000;60:7133–41; 262. *Clin Cancer Res* 2003;9:2826–36; 263. *Cancer Sci* 2004;95:44–51; 264. *Cancer Res* 2000;60:2805–9; 265. *Cell Mol Life Sci* 2002;59:1406–12; 266. *Cancer Res* 2000;60:4386–90; 267. *Oncogene* 2002;21:8843–51; 268. *Cancer Res* 2001;61:348–54; 269. *Cancer Res* 1993;53:4443–8; 270. *Breast Cancer Res Treat* 1993;26:23–39; 271. *Eur J Biochem* 1996;237:653–9; 272. *Cancer Res* 1997;57:2661–7; 273. *Breast Cancer Res Treat* 1999;56:187–96.

Irinotecan pharmacokinetics/pharmacodynamics and UGT1A genetic polymorphisms in Japanese: roles of UGT1A1*6 and *28

Hironobu Minami[a], Kimie Sai[b,c], Mayumi Saeki[b], Yoshiro Saito[b,d], Shogo Ozawa[b,e], Kazuhiro Suzuki[c], Nahoko Kaniwa[b,f], Jun-ichi Sawada[b,d], Tetsuya Hamaguchi[g], Noboru Yamamoto[g], Kuniaki Shirao[g], Yasuhide Yamada[g], Hironobu Ohmatsu[h], Kaoru Kubota[h], Teruhiko Yoshida[i], Atsushi Ohtsu[j] and Nagahiro Saijo[k]

Objectives SN-38, an active metabolite of irinotecan, is detoxified by glucuronidation with UGT1A isoforms, 1A1, 1A7, 1A9, and 1A10. The pharmacogenetic information on UGT1A haplotypes covering all these isoforms is important for the individualized therapy of irinotecan. Associations between UGT1A haplotypes and pharmacokinetics/ pharmacodynamics of irinotecan were investigated to identify pharmacogenetic markers.

Methods Associations between UGT1A haplotypes and the area under concentration curve ratio (SN-38 glucuronide/ SN-38) or toxicities were analyzed in 177 Japanese cancer patients treated with irinotecan as a single agent or in combination chemotherapy. For association analysis, diplotypes of UGT1A gene segments [(1A1, 1A7, 1A9, 1A10), and Block C (common exons 2–5)] and combinatorial haplotypes (1A9-1A7-1A1) were used. The relationship between diplotypes and toxicities was investigated in 55 patients treated with irinotecan as a single agent.

Results Among diplotypes of UGT1A genes, patients with the haplotypes harboring UGT1A1*6 or *28 had significantly reduced area under concentration curve ratios, with the effects of UGT1A1*6 or *28 being of a similar scale. A gene dose effect on the area under concentration curve ratio was observed for the number of haplotypes containing *28 or *6 (5.55, 3.62, and 2.07 for 0, 1, and 2 haplotypes, respectively, $P < 0.0001$). In multivariate

analysis, the homozygotes and double heterozygotes of *6 and *28 (*6/*6, *28/*28 and *6/*28) were significantly associated with severe neutropenia in 53 patients who received irinotecan monotherapy.

Conclusions The haplotypes significantly associated with reduced area under concentration curve ratios and neutropenia contained UGT1A1*6 or *28, and both of them should be genotyped before irinotecan is given to Japanese and probably other Asian patients. *Pharmacogenetics and Genomics* 17:497–504 © 2007 Lippincott Williams & Wilkins.

Introduction

Irinotecan, an anticancer prodrug, is widely applied for colorectal, lung, stomach, ovarian, and other various cancers. It is activated by carboxylesterases to SN-38 (7-ethyl-10-hydroxycamptothecin), which shows antitumor activity by inhibiting topoisomerase I [1,2]. SN-38 is subsequently glucuronidated by uridine diphosphate glucuronosyltransferases (UGTs) to form an inactive metabolite, SN-38 glucuronide (SN-38G) [3]. Dose-limiting toxicities of irinotecan are diarrhea and leukopenia [4], and reduced activity for SN-38G formation is closely related to severe toxicities [5]. Among UGT isoforms, UGT1A1 is abundant in both the liver and intestine and is thought to be mainly responsible for inactivation of SN-38 [3,6]. Genetic polymorphisms of UGT1A1 result in reduced enzyme activity and increased toxicity by irinotecan. A significant association of UGT 1A1*28, a repeat polymorphism of the TATA box (-40_-39insTA) [3,7], with severe irinotecan-induced diarrhea/leukopenia was first reported in a retrospective study of Japanese cancer patients [8]. Subsequent pharmacogenetic studies in Caucasians have shown close associations of *28 with reduced glucuronidation of SN-38 and/or severe neutropenia/diarrhea [9–12]. These

studies have clearly indicated that *28 is a good genetic marker for individualized irinotecan therapy. On the basis of these observations, the Food and Drug Administration of the United States has approved an amendment of the label for Camptosar (irinotecan HCl) and added a warning to consider a reduction in the starting dose of irinotecan for *28 homozygous patients (NDA 20-571/S-024/S-027/S-028).

There is significant racial difference in UGT1A1 polymorphisms among Asians, Caucasians, and Africans [13]. Although the association of UGT 1A1*28 with toxicities by irinotecan was first described in Japanese patients, its frequency in Japanese is one-third of that in Caucasians. Another low-activity allele *6 [211G > A(G71R)], which is not detected in Caucasians or Africans, is as frequent as the *28 allele in Japanese. Moreover, the area under concentration curve (AUC) ratio of SN-38G to SN-38 was decreased in patients having *6 haplotypes [14].

In addition to UGT1A1, recent studies have suggested possible contributions to SN-38G formation by UGT1A7, 1A9, and 1A10 [15–17], which are expressed in the gastrointestinal tract, the liver and intestine, and extrahepatic tissues, respectively [18]. Altered activity resulted from genetic polymorphisms of these isoforms, including 1A7*3 [387T > G(N129K), 391C > A(R131K), 622T >C(W208R)], 1A9*22 (-126_-118T$_9$ > T$_{10}$), 1A9*5 [766G >A(D256N)], and UGT1A10*3 [605C > T(T202I)], but clinical relevance of these polymorphisms is yet to be elucidated [16,19–24]. Moreover, close linkages among 1A9, 1A7, and 1A1 polymorphisms were found in Caucasians and Asians in an ethnic-specific manner [20,25–27]. Therefore, comprehensive investigation that covers these genes, along with linkages among the polymorphisms, is needed, in each ethnic population, to evaluate associations between the genetic polymorphisms and pharmacokinetics, as well as clinical outcomes of irinotecan therapy.

Recently, we have analyzed the segmental and block haplotypes of 1A8, 1A10, 1A9, 1A7, 1A6, 1A4, 1A3 and 1A1, and the common exons 2–5 (Block C) in a Japanese population, including the 177 cancer patients treated with irinotecan, and showed close linkages between the haplotypes, that is, 1A9*22 and 1A7*1, 1A7*3 and 1A1*6, and 1A7*3 and 1A1*28 [28]. Preliminary results of UGT1A1 pharmacogenetics on 85 of these cancer patients were reported previously [14]. In the current study, we investigated the pharmacogenetics of irinotecan, focusing on diplotypes of the UGT1A complex covering 1A1, 1A7, 1A9, 1A10, and Block C (exons 2–5) of 177 patients, so as to elucidate haplotypes or genetic markers associated with altered glucuronidation of SN-38 and toxicities.

Methods

Patients and treatment schedule

Patients with cancers who started chemotherapy with irinotecan at two National Cancer Center Hospitals

(Tokyo and Kashiwa, Japan) were eligible if they had not received irinotecan previously. Other eligibility criteria included bilirubin ≤ 2 mg/dl, aspartate aminotransferase (GOT) ≤ 105 IU/l, alanine aminotransferase (GPT) ≤ 120 IU/l, creatinine ≤ 1.5 mg/dl, white blood cell count ≥ 3000/μl, performance status of 0–2, and at least 4 weeks after the last chemotherapy (2 weeks for radiotherapy). Exclusion criteria were diarrhea, active infection, intestinal paralysis or obstruction, and interstitial pneumonitis. The ethics committees of the National Cancer Center and the National Institute of Health Sciences approved this study, and written informed consent was obtained from all participants.

Irinotecan was administered as a single agent or in combination chemotherapy at the discretion of attending physicians. Doses and schedules were according to approved usage in Japan; intravenous 90-min infusion at a dose of 100 mg/m^2 weekly or 150 mg/m^2 biweekly. In terms of combination chemotherapy, the dose of irinotecan was reduced according to clinical protocols.

Genetic polymorphisms of UGT1As and pharmacokinetics

Detailed assay methods for genotypes of the UGT1A gene complex were reported previously [14,28]. In this study, we focused on the genetic variations in UGT1A1, 1A7, 1A9, and 1A10 and common exons 2–5, as they have been reported to contribute to the SN-38 glucuronidation. Haplotype analysis covering these regions was performed in our previous study [28], and haplotypes of each UGT1A segment [exon 1 for 1A1, 1A7, 1A9, or 1A10; and Block C (common exons 2–5)] are summarized in Fig. 1.

Pharmacokinetic analysis for irinotecan was performed as described previously [14]. Briefly, heparinized blood was collected before administration of irinotecan, as well as 0 and 20 min, and 1, 2, 4, 8, and 24 h after termination of the first infusion of irinotecan. Plasma concentrations of irinotecan, SN-38 and SN-38G were determined by the high-performance liquid chromatography [29], and AUC was calculated by the trapezoidal method using WinNonlin version 4.01 (Pharsight Corporation, Mountain View, California, USA). Associations between genotypes and the AUC ratio (AUC of SN-38G/AUC of SN-38) were evaluated in 176 patients.

Monitoring and toxicities

A complete medical history and data on physical examinations were recorded before the irinotecan therapy. Complete blood cell counts with differentials and platelet counts, as well as blood chemistry, were measured once a week during the first 2 months of irinotecan treatment. Toxicities were graded according to the Common Toxicity Criteria of National Cancer Institute version 2. Association of genetic factors with irinotecan toxicities was analyzed primarily in patients who received irinotecan as a single agent.

Fig. 1

UGT1A1

Region	Enhancer	Promoter	Exon 1		Frequency
Nucleotide change	-3279 T>G	-40_-39 insTA	211 G>A	686 C>A	
Amino acid change			G71R	P229Q	
Marker allele	*60	*28	*6	*27	

Haplotype						Frequency
*1						0.548
*6						0.167
*60						0.147
*28	*28b					0.138
	*28c					
	*28d					

UGT1A10

Region	Exon 1				Frequency
Nucleotide change	4 G>A	177 G>A	200 A>G	605 C>T	
Amino acid change	A2T	M59I	E67G	T202I	
Marker allele	*2T	*2	*67G	*3	

Haplotype					Frequency
*1					0.981
*2					0.006
*2T					0.003
*3					0.010
*67G					0.000

UGT1A7

Region	Exon 1				Frequency
Nucleotide change	387 T>G	391C>A	392 G>A	622 T>C	
Amino acid change	N129K	R131K		W208R	
Marker allele	*2,*3	*2,*3	*2,*3	*3,*4	

Haplotype					Frequency
*1					0.630
*2					0.147
*3					0.223

Block C

Region	Exon.4	Exon.5		3'-UTR			Frequency
Nucleotide change	1091 C>T	1456 T>G	1598 A>C	*211(1813) C>T	*339 (1941) C>G	*440(2042) C>G	
Amino acid change	P364L	Y486D	H533P				
Marker allele	*364L	*7	*533P	*IB	*IB	*IB	

Haplotypes								Frequency
*IA								0.864
*IB	*1b–*1j							0.127
	*533P							
*7								0.003
*364L								0.006

UGT1A9

Region	Promoter		Exon1			Frequency
Nucleotide change	-126_-118 T9>T10	-126_-118 T9>T11	422 C>G	726 T>G	766 G>A	
Amino acid change			S141C	Y242X	D256N	
Marker allele	*22	*T11	*141C	*4	*5	

Haplotype						Frequency
*1						0.347
*22						0.644
*141C						0.000
*4						0.000
*5						0.006
*T11						0.003

Haplotypes of UGT1A gene segments (UGT1A1, 1A7, 1A9, 1A10, and Block C) in 177 Japanese cancer patients. The tagging variations and haplotypes are shown. Variant alleles are indicated in grey. Definition of Block C haplotypes in our previous paper ([14]) (corresponding to Block 2) were slightly modified.

Statistical analysis

Statistical analysis on the differences in the AUC ratios (SN-38G/SN-38) among UGT1A genotypes was performed using the Kruskal–Wallis test, followed by nonparametric Dunnett's multiple comparison test, or with Wilcoxon test. Analysis of a gene–dose effect of each haplotype was performed using the Jonckheere–Terpestra test in the SAS system, version 5.0 (SAS Institute, Cary, North Carolina, USA). Relationship of UGT1A genetic polymorphisms to the toxicities of irinotecan was assessed by the χ^2 test via the use of using Prism version 4.0 (GraphPad Prism Software, San Diego, California, USA). The P-value of 0.05 (two-tailed) was set as a significant level, and the

multiplicity adjustment was conducted for pharmacokinetics data with the false discovery rate [30].

To identify factors associated with the log-transformed AUC ratio of SN-38G/SN-38, multiple regression analysis was performed using age, sex, body surface area, dosage of irinotecan, history of smoking or drinking, performance status, coadministered drugs, serum biochemistry parameters at baseline, and 1A9-1A7-1A1 and Block C haplotypes (five or more chromosome numbers) or '1A1*6 or *28'. For multiple regression analysis of neutropenia, variables included the absolute neutrophil count at baseline and the dosing interval, in addition to

the other patient background factors described above. The multivariate analyses were performed by using JMP version 6.0.0 software (SAS Institute). The variables in the final models for both AUC ratio and neutropenia were chosen by forward and backward stepwise procedures at significance levels of 0.25 and 0.05, respectively.

Results

Patients and UGT1A haplotypes

Patient demographics and information on the treatment are summarized in Table 1. In addition to UGT1A1, UGT1A7, 1A9, and 1A10 were also reported to glucuronidate SN-38 [15–17]. In our previous study, haplotype analysis covering the 1A9 to 1A1 (5′–3′) gene segments was conducted, and the combinatorial diplotypes (1A9-1A7-1A1) of the patients were determined. It must be noted that close linkages between 1A9*22 and 1A7*1, between 1A7*2 and 1A1*60, and between 1A7*3 and 1A1*6 or 1A1*28 were observed as described previously [28]. To clarify the linkages between these segmental haplotypes (1A9, 1A7, and 1A1), we grouped the combinatorial (1A9-1A7-1A1) haplotypes into four categories (A–D) based on the 1A1 haplotypes (*1, *6, *60, and *28). Each group was further divided into the subgroups based on the previously defined Block 9/6 (including 1A9, 1A7, and 1A6) haplotypes (Table 2). The frequency of Group B haplotypes (B1-B4) harboring 1A1*6 was 0.167 and higher than that of Group D haplotypes (D1-D6) with *28 (0.138) in this population.

Association of 1A9-1A7-1A1 diplotypes to SN-38G formation

When relationship between the UGT1A diplotypes (1A9-1A7-1A1) and the SN-38G/SN-38 AUC ratio was analyzed

in the 176 cancer patients the AUC ratio for the diplotypes of B2/B2, D2/A1, and D1/B2 was statistically significantly lower than the A1/A1 diplotype (Fig. 2). These diplotypes harbored 1A1*6, *28 or both. Significant gene–dose effects of B2 (among A1/A1, B2/A1, and B2/B2) and C3 (among A1/A1, C3/A1, and C3/C3) were also observed (Fig. 2). As no significant differences in AUC ratios were observed between D1/A1 and D2/A1, D1/C3 and D2/C3, and D1/B2 and D2/B2, the haplotype combination 1A9*1-1A7*3 or 1A9*22-1A7*1 was not influential on the AUC ratio.

As the effect of diplotypes harboring UGT1A1 polymorphism was prominent, we grouped the whole gene (1A9-1A7-1A1) diplotypes according to the 1A1 diplotypes (the upper part of Fig. 2). Patients with *6 or *28 (except for *28/*28) haplotypes had significantly lower AUC ratios than the wild-type (*1/*1), and significant gene–dose effects were observed for *28 (among *1/*1, *28/*1, and *28/*28) and *6 (among *1/*1, *6/*1 and *6/*6). A significant additive effect of *6 and *28 on the decreased AUC ratio was also observed when the values for *28/*1 were compared with those for *28/*6 (Fig. 2 and Table 3).

Regarding other polymorphisms, a statistically nonsignificant tendency to decrease the AUC ratio was observed for *60

Table 1　Characteristics of Japanese cancer patients in this study

		No. of participants	
Age			
Mean/range	60.5/26–78	177	
Sex			
Male/female		135/42	
Performance status	0/1/2	84/89/4	
Combination therapy and tumor type (initial dose of irinotecan; mg/m²)			
Irinotecan monotherapy	Lung (100)	21	
	Colon (150)	28	
	Others (100)	7	
With platinum-containing drug[a]	Lung (60)	58[b]	48 [60][c]
	Stomach (70)	9	9 [80][c]
	Others (60)	5	5 [80][c]
With 5-fluorouracil (including tegafur)	Colon (100 or 150)	34	
	Others (90 or 100)	2	
With mitomycin-C	Stomach (150)	10	
	Colon (150)	1	
With amrubicin	Lung (60)	2	
Previous treatment			
Surgery	Yes/no	85/92	
Chemotherapy	Yes/no	97/80	
Radiotherapy	Yes/no	26/151	
Smoking history	Yes/no	29/148	

[a]Cisplatin, cisplatin plus etoposide or carboplatta.
[b]Two and eight patients received cisplatin and etoposide and carboplatin, respectively.
[c]Number of cisplatin-administered patients [initial dose of cinlatin (mg/m²) is shown in brackets].

Table 2　Combinatorial haplotypes covering UGT1A9, UGT1A7, and UGT1A1

Haplotype	Block haplotype[a]			Combination of segmental haplotypes	Cancer patients	
	Block 9/6	Block 4	Block 3/1	1A9-1A7-1A1	N[b]	Frequency
A1[c]	*I	*1	*I	*22-*1-*1	189	0.534
	*I	*3	*I			
A3	*III	*1	*I	*1-*2-*1	2	0.006
A2	*II	*1	*I	*1-*3-*1	1	0.003
A4	*IV	*1	*I	*22-*3-*1	1	0.003
A5				*T11-*1-*1	1	0.003
B2[c]	*II	*1	*III			
	*II	*1	*VI	*1-*3-*6	47	0.133
	*II	*4	*VI			
B4	*IV	*1	*III	*22-*3-*6	6	0.017
B1	*I	*1	*III	*22-*1-*6	5	0.014
	*I	*1	*VI			
B3	*III	*1	*III	*1-*2- *6	1	0.003
C3[c]	*III	*3	*IV			
	*III	*1	*IV			
	*III	*3	*V	*1-*2-*60	44	0.124
	*III	*1	*V			
C1	*I	*3	*IV	*22-*1-*60	5	0.014
	*I	*1	*IV			
C2	*II	*3	*IV	*1-*3-*60	2	0.006
C7	*VII	*3	*V	*22-*2-*60	1	0.003
D1	*I	*1	*IIa	*22-*1-*28	23	0.065
	*I	*1	*IIc			
D2	*II	*1	*IIa			
	*II	*3	*IIa	*1-*3-*28	22	0.062
	*II	*1	*IIc			
D6	*VI	*1	*IIb	*1-*2-*28	4	0.011
				Total	354	1.000

[a]Block haplotypes described in Ref. [28] are shown for reference. 1A9 and 1A7 are included in block 9/6 and 1A1 is included in block 3/1.
[b]Number of chromosomes.
[c]Major combinatrial haplotypes.

Fig. 2
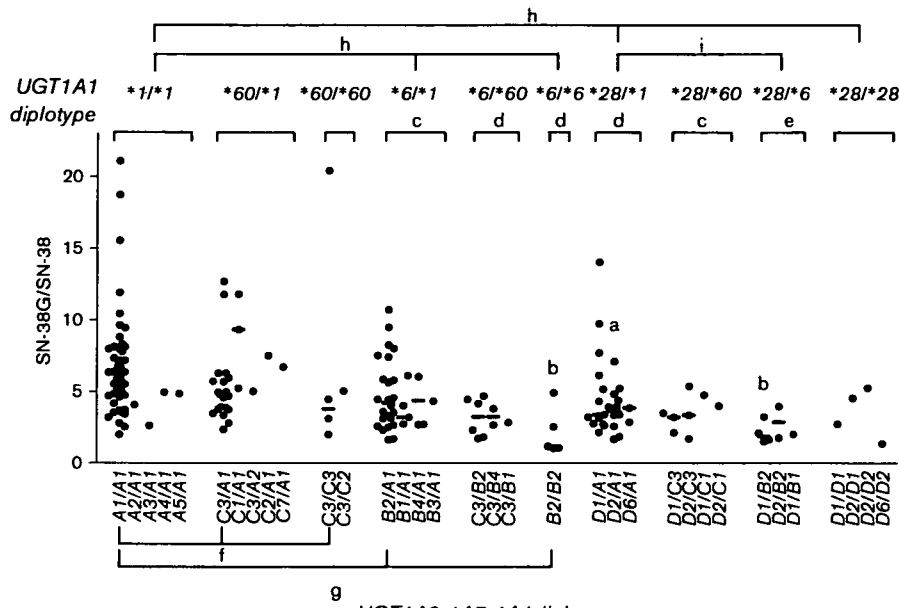
g
UGT1A9-1A7-1A1 diplotype
The association of *UGT1A* diplotypes with the reduced area under concentration curve (AUC) ratio (SN-38G/SN-38) in 176 Japanese cancer patients who received irinotecan. The whole gene (*1A9-1A7-1A1*) diplotypes are shown below the abscissa and the *UGT1A1* diplotypes are indicated in the upper part of the figure. Each point represents a patient value, and the median is indicated by a bar. Significant reductions in the AUC ratio were detected in the *B2/B2*, *D2/A1*, and *D1/B2* compared with *A1/A1* for the whole gene diplotypes [Kruskal–Wallis test (*P*=0.0009) followed by Dunnett's multiple comparison test]. As for the *1A1* diplotypes, significant reductions were detected in the *6/*1*, *6/*60*, *6/*6*, *28/*1*, *28/*60*, and *28/*6* compared with the *1/*1* group [Kruskal–Wallis test (*P*<0.0001) followed by Dunnett's multiple comparison test]. Gene–dose effects on the reduced AUC ratio were significant for *6 and *28 (Jonckheere–Terpestra test). A significant additive effect of *6 on the reduced AUC ratio by *28 was detected by comparing *28/*1 and *28/*6. [a]*P*<0.05 and [b]*P*<0.01 against *A1/A1* group (Dunnett's multiple comparison test); [c]*P*<0.05, [d]*P*<0.01, and [e]*P*&<0.001 against the *1/*1* group (Dunnett's multiple comparison test); [f]*P*<0.05, [g]*P*<0.001, and [h]*P*<0.0001 (Jonckheere–Terpestra test for gene–dose effect); [i]*P*<0.01 (Wilcoxon test).

(*P* = 0.1134). No significant effects on the AUC ratio were observed for Block C (exon 2–5) haplotypes or rare variations including *1A10* (*2T*, *2*, or *3*) and *1A9* (*5*, *T11*).

Multiple regression analysis of the area under concentration curve ratio

We further assessed the impact of *UGT1A* genetic factors on the AUC ratio by multiple regression analysis. First, we used the *1A9-1A7-1A1* and Block C haplotypes as genetic factors. The AUC ratio was significantly associated with the haplotypes *B2*, *D1*, and *D2* and serum biochemistry parameters indicating hepatic or renal function before treatment. The Groups B and D haplotypes harbor *1A1*6* and *28*, respectively. The dependency on specific *1A7* or *1A9* polymorphisms, however, was not obtained, considering the contributions of both *D1* and *D2*. As *1A1*6* and *28* are mutually exclusive and their effects are comparable, we grouped *1A1*6* and *28* into the same category in the final multiple regression model (Table 4). The final model confirmed the significant contribution of this genetic marker (*6* or *28*) to the AUC ratio.

Effects of the genetic marker '*6 or *28' on pharmaco kinetic parameters

Then, a dose effect of the genetic marker '*6 or *28' on pharmacokinetic parameters was further analyzed

Table 3 AUC ratio of SN-38 glucuronide to SN-38 for *UGT1A* diplotypes

| Diplotype | Number of patients | AUC ratio | | P-value[a] (vs. *1/*1) |
		Median	Interquartile range	
*1/*1	55	6.13	4.72–7.79	
*1/*60	25	5.04	3.85–6.52	0.9803
*60/*60	5	4.48	2.57–12.74	0.8141
*6/*1	32	4.03	2.74–5.97	0.0126
*6/*60	9	2.84	2.09–4.33	0.0021
*6/*6	5	1.19	1.06–3.74	0.0012
*28/*1	26	3.65	2.76–5.21	0.0040
*28/*60	8	3.44	2.68–4.40	0.0261
*28/*6	7	2.03	1.65–3.26	<0.0001
*28/*28	4	3.65	2.05–4.92	0.2322

AUC, area under concentration curve.
[a]Dunnett's multiple comparison test.

(Fig. 3). Patients with one haplotype harboring either *6 or *28 (*6/*1*, *6/*60*, *28/*1*, and *28/*60*) had lower SN-38G/SN-38 AUC ratios (median, 3.62; interquartile range, 2.74–5.18) than patients without *6 or *28 (*1/*1*, *60/*1*, and *60/*60*) (5.55, 4.13–7.26), and patients with two haplotypes harboring *6 or *28 (*6/*6*, *28/*28*, and *28/*6*) had the lowest AUC ratio (2.07, 1.45–3.62) (*P* < 0.0001, Fig. 3a). Similarly, the number of the *6 or *28-containing haplotypes affected the AUC ratios of SN-38 to irinotecan (Fig. 3b). When the correlations

between irinotecan dosage and the AUC of SN-38 were tested, different correlations were obtained according to the number of the haplotypes (Fig. 3c). The slope of regression line for one and two haplotypes harboring *6 or *28 was 1.4-fold and 2.4-fold greater, respectively, than that for the diplotype without *6 or *28.

Associations of UGT1A1 genetic polymorphisms with toxicities

Association between genetic polymorphisms and toxicities was investigated in patients receiving irinotecan as a single agent. One patient was referred to another hospital 3 days after the first administration of irinotecan without evaluating toxicities and was lost in terms of follow-up. Therefore, association between genetic polymorphisms and toxicities was investigated in 55 patients. Six (11%) and 14 (25%) patients experienced grade 3 or greater diarrhea and neutropenia, respectively. As for the 1A9-1A7-1A1 diplotypes, a higher incidence of grade 3 or greater neutropenia was observed in D1/B2 (1A1*28/*6) (100%, n = 3) than in A1/A1 (11.8%, n = 17) (P = 0.0088, Fisher's exact test), indicating clinical impact of the genetic marker 1A1*6 or *28. As for the dose effect of '*6 or *28', incidences of grade 3 or 4 neutropenia were 14, 24, and 80% for 0, 1, and 2 haplotypes harboring these markers, respectively (Table 5). A significant association between '*6 or *28'and neutropenia was also observed for 62 patients who received irinotecan in combination with cisplatin (Table 5). No association, however, was observed between diarrhea and the marker '*6 or *28'.

Multivariate analysis for irinotecan toxicities

We further evaluated the effect of the genetic marker '*6 or *28' on neutropenia in multivariate analysis, and confirmed a significant correlation of '*6 or *28' with the nadir of absolute neutrophil counts (Table 6). Elevated alkaline phosphatase levels and the absolute neutrophil count at baseline were also significant.

Discussion

The association study with the 1A9-1A7-1A1 diplotypes revealed that the reduction in inactivation of SN-38, as well

Table 4 Multiple regression analysis toward the AUC ratio (SN-38G/SN-38)[a]

Variable	Coefficient	F-value	P-value	R^2	Intercept	N
				0.410	0.8869	176
*6 or *28	−0.189	70.2	<0.0001			
Age	0.005	8.88	0.0033			
Serum albumin level[b]	−0.136	9.92	0.0019			
Serum GOT and ALP[c]	0.070	8.88	0.0033			
Serum creatinine[d]	0.210	7.23	0.0079			

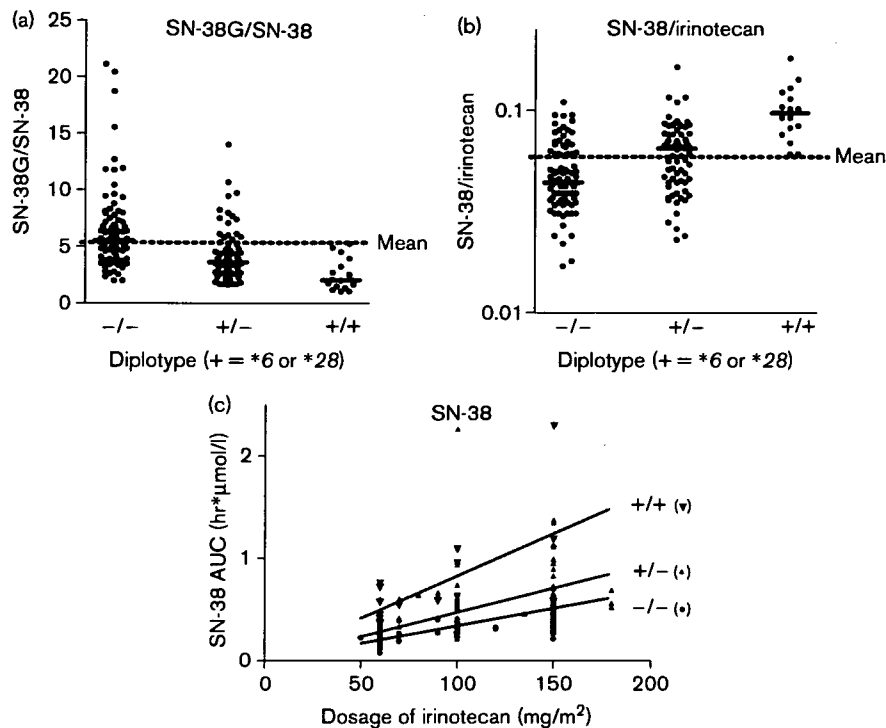ALP, alkaline phosphatase; AUC, area under concentration curve.
[a]The values after logarithmic conversion were used as an objective variable.
[b]The absolute value (g/dl) before irinotecan treatment.
[c]Grade 1 or greater scores in both serum GOT and ALP before irinotecan treatment.
[d]Grade 1 or greater scores in serum creatinine before irinotecan treatment.

as neutropenia, was dependent on the Groups B and D haplotypes which corresponded to the 1A1*6 and *28 segmental haplotypes. Also, multivariate analyses clearly showed clinical significance of the genetic marker '*6 or *28' for both pharmacokinetics and toxicity of irinotecan in Japanese patients (Tables 3 and 6). UGT1A1*6 and *28 were mutually exclusive [14] and contributed to the reduction in glucuronidation of SN-38 to the same extent. Therefore, the activity of SN-38 glucuronidation in individuals depended on the number of the haplotypes harboring *6 or *28. Although the role of 1A1*28 for irinotecan toxicity has been focused on [8–12], this study strongly suggests that *6 should be tested in addition to *28 before starting chemotherapy with irinotecan in Japanese patients.

The clinical importance of *6 for neutropenia by irinotecan was also supported by a recent report in Korean patients who received irinotecan and cisplatin [31]. Although no patients with irinotecan as a single agent were homozygous for *6 in our study, clinical significance of the double heterozygote, *6/*28, was clearly demonstrated. Among patients treated with irinotecan in combination chemotherapy, the majority of patients received platinum agents in our study. A significant association of '*6 or *28' with a higher incidence of grade 3 or 4 neutropenia was also observed in patients who received irinotecan and cisplatin (Table 5). These findings further support the necessity of testing '*6 or *28' before irinotecan is given to patients.

As possible enhancement of toxicities by the *27 allele was suggested [8], we evaluated the effect of the *28c haplotype, which had an additional single-nucleotide polymorphism [*27; 686C > A(P229Q)] to the *28 allele (-40_-39insTA). In our cohort of patients, there were three *28c heterozygotes (*28c/*1) and one double heterozygote (*28b/*28c). The values of the AUC ratio were within the range of variations of the *28 group, and no additional impact of *28c was observed in relation to toxicities.

Although the decreasing trend of the AUC ratio for 1A1*60 (and combinatorial haplotype C3) was observed (Fig. 2), the contribution of 1A1*60 to toxicities was not clearly demonstrated in this study as reported in the Japanese retrospective study [32].

In addition to UGT1A1, recent studies have suggested possible contributions of UGT1A7, 1A9, and 1A10 to SN-38G formation [15–17]. An in-vitro study demonstrated that 1A7*3 [387T > G(N129K), 391C > A(R131K), 622T > C(W208R)] had reduced activity in terms of SN-38G formation [16]. Results of clinical studies, however, on the association between 1A7 polymorphisms and irinotecan toxicity/efficacy are inconsistent, whereas different populations with different combination therapies were used [19,20]. Furthermore, it was reported that the UGT1A7 polymorphisms (*2 and *3), which were linked to 1A9*1, were associated with a lowered incidence

Fig. 3

Effects of the genetic marker of *UGT1A1* '*6 or *28'* on the area under concentration curve (AUC) ratios of SN-38G/SN-38 (a) and SN-38/irinotecan (b), and SN-38 by irinotecan dosage (c) in 176 Japanese cancer patients after irinotecan treatment.

Table 5 Association of *UGT1A1*6* and *28* with irinotecan toxicities

Diplotype (+ = *6 or *28)	Number of patients	Diarrhea (grade 3)	Neutropenia (grade 3 or 4)
Irinotecan monotherapy			
− / −	21	3 (14.3%)[a]	3 (14.3%)
+ / −	29	2 (6.90%)	7 (24.1%)
+ / +	5	1 (20.0%)	4 (80.0%)
P-value[b]		0.8500	**0.0117**
P-value[c]		0.3889	**0.0124**
With cisplatin			
− / −	35	1 (2.9%)	20 (57.1%)
+ / −	20	2 (10.0%)	14 (70.0%)
+ / +	7	1 (14.3%)	7 (100%)
P-value[b]		0.1747	**0.0315**
P-value[c]		0.3886	0.0863

[a]Percentage of the patient number in each diplotype is indicated in parentheses.
[b]Chi-squared test for trend.
[c]Fisher's exact test, (−/− and +/−) vs. +/+.

of diarrhea in the irinotecan/capecitabine regimen, in which diarrhea was a major toxicity [20]. A highly frequent allele *1A9*22* with an insertion of T into the nine T repeats in the promoter region (-126_-118T$_9$ > T$_{10}$) was shown to have an enhanced promoter activity in an in-vitro reporter assay [21], whereas 1A9 protein expression levels did not change in the clinical samples [22]. Rare variations, *1A9*5* [766G > A(D256N)] and *UGT1A10*3* [605C > T(T202I)], were shown to cause reduced activity in vitro, but their clinical importance is still unknown [23,24]. Moreover, close linkages among *1A9*, *1A7*, and *1A1*

Table 6 Multiple regression analysis of the nadir of absolute neutrophil counts in the patients with irinotecan monotherapy

Variable	Coefficient	F-value	P-value	R²	Intercept	N
				0.3942	643	53
Serum ALP[a]	−349.9	12.2	0.0010			
Neutrophil count before irinotecan treatment	0.2466	13.5	0.0006			
*6 or *28	−369.1	6.40	0.0146			

[a]Grade 1 or greater scores of serum ALP before irinotecan treatment.

polymorphisms were found in Caucasians and Asians in an ethnic-specific manner [20,25–28].

Our study also revealed close linkages between *1A9*22* and *1A7*1*, *1A7*3* and *1A1*6* or *28* [28]. This fact makes it difficult to draw firm conclusions about the effects of *1A7*3* and *1A9*22* themselves. It is, however, reasonable to conclude that the degree of neutropenia depends on the activity of UGT1A1, because UGT1A1 is a major UGT1A enzyme in the liver and plays a primary role for regulating plasma concentrations of SN-38.

Taken together, for practical application to individualized irinotecan therapy, genotyping of *UGT1A1*6* and *28* would be beneficial and necessary in Japanese cancer patients to avoid severe adverse reactions. The frequency

of homozygotes for '*6 or *28' (namely, *6/*6, *6/*28, and *28/*28) is approximately 10%, which is comparable to the frequency of *28 homozygotes in Caucasian populations. In our study, it may be difficult to establish definite guidelines for dose reductions of irinotecan for patients homozygous for '*6 or *28'. Considering, however, 2.4-fold steep relationship between the dose of irinotecan and the AUC of SN-38 for patients homozygous for '*6 or *28' compared with patients without '*6 or *28' (Fig. 3c), the dose for patients homozygous for '*6 or *28' should be reduced to a half of the dosage recommended for other patients. Prospective studies are necessary to confirm the validity of the recommendation for dose reduction in Japanese cancer patients homozygous for '*6 or *28'.

References
1 Garcia-Carbonero R, Supko JG. Current perspectives on the clinical experience, pharmacology, and continued development of the camptothecins. *Clin Cancer Res* 2002; 8:641–661.
2 Slatter JG, Su P, Sams JP, Schaaf LJ, Wienkers LC. Bioactivation of the anticancer agent CPT-11 to SN-38 by human hepatic microsomal carboxylesterases and the in vitro assessment of potential drug interactions. *Drug Metab Dispos* 1997; 25:1157–1164.
3 Iyer L, King CD, Whitington PF, Green MD, Roy SK, Tephly TR, et al. Genetic predisposition to the metabolism of irinotecan (CPT-11). Role of uridine diphosphate glucuronosyltransferase isoform 1A1 in the glucuronidation of its active metabolite (SN-38) in human liver microsomes. *J Clin Invest* 1998; 101:847–854.
4 De Forni M, Bugat R, Chabot GG, Culine S, Extra JM, Gouyette A, et al. Phase I and pharmacokinetic study of the camptothecin derivative irinotecan, administered on a weekly schedule in cancer patients. *Cancer Res* 1994; 54:4347–4354.
5 Gupta E, Lestingi TM, Mick R, Ramirez J, Vokes EE, Ratain MJ. Metabolic fate of irinotecan in humans: correlation of glucuronidation with diarrhea. *Cancer Res* 1994; 54:3723–3725.
6 Hanioka N, Ozawa S, Jinno H, Ando M, Saito Y, Sawada J. Human liver UDP-glucuronosyltransferase isoforms involved in the glucuronidation of 7-ethyl-10-hydroxycamptothecin. *Xenobiotica* 2001; 31:687–699.
7 Fisher MB, VandenBranden M, Findlay K, Burchell B, Thummel KE, Hall SD, et al. Tissue distribution and interindividual variation in human UDP-glucuronosyltransferase activity: relationship between UGT1A1 promoter genotype and variability in a liver bank. *Pharmacogenetics* 2000; 10:727–739.
8 Ando Y, Saka H, Ando M, Sawa T, Muro K, Ueoka H, et al. Polymorphisms of UDP-glucuronosyltransferase gene and irinotecan toxicity: a pharmacogenetic analysis. *Cancer Res* 2000; 60:6921–6926.
9 Iyer L, Das S, Janisch L, Wen M, Ramirez J, Karrison T, et al. UGT1A1*28 polymorphism as a determinant of irinotecan disposition and toxicity. *Pharmacogenomics J* 2002; 2:43–47.
10 Innocenti F, Undevia SD, Iyer L, Chen PX, Das S, Kocherginsky M, et al. Genetic variants in the UDP-glucuronosyltransferase 1A1 gene predict the risk of severe neutropenia of irinotecan. *J Clin Oncol* 2004; 22:1382–1388.
11 Marcuello E, Altes A, Menoyo A, del Rio E, Gomez-Pardo M, Baiget M. UGT1A1 gene variations and irinotecan treatment in patients with metastatic colorectal cancer. *Br J Cancer* 2004; 91:678–682.
12 Rouits E, Boisdron-Celle M, Dumont A, Guerin O, Morel A, Gamelin E. Relevance of different UGT1A1 polymorphisms in irinotecan-induced

13 Kaniwa N, Kurose K, Jinno H, Tanaka-Kagawa T, Saito Y, Saeki M, et al. Racial variability in haplotype frequencies of UGT1A1 and glucuronidation activity of a novel single nucleotide polymorphism 686C>T (P229L) found in an African-American. *Drug Metab Dispos* 2005; 33:458–465.
14 Sai K, Saeki M, Saito Y, Ozawa S, Katori N, Jinno H, et al. UGT1A1 haplotypes associated with reduced glucuronidation and increased serum bilirubin in irinotecan-administered Japanese patients with cancer. *Clin Pharmacol Ther* 2004; 75:501–515.
15 Ciotti M, Basu N, Brangi M, Owens IS. Glucuronidation of 7-ethyl-10-hydroxycamptothecin (SN-38) by the human UDP-glucuronosyltransferases encoded at the UGT1 locus. *Biochem Biophys Res Commun* 1999; 260:199–202.
16 Gagne JF, Montminy V, Belanger P, Journault K, Gaucher G, Guillemette C. Common human UGT1A polymorphisms and the altered metabolism of irinotecan active metabolite 7-ethyl-10-hydroxycamptothecin (SN-38). *Mol Pharmacol* 2002; 62:608–617.
17 Oguri T, Takahashi T, Miyazaki M, Isobe T, Kohno N, Mackenzie PI. UGT1A10 is responsible for SN-38 glucuronidation and its expression in human lung cancers. *Anticancer Res* 2004; 24:2893–2896.
18 Basu NK, Ciotti M, Hwang MS, Kole L, Mitra PS, Cho JW, et al. Differential and special properties of the major human UGT1-encoded gastrointestinal UDP-glucuronosyltransferases enhance potential to control chemical uptake. *J Biol Chem* 2004; 279:1429–1441.
19 Ando M, Ando Y, Sekido Y, Ando M, Shimokata K, Hasegawa Y. Genetic polymorphisms of the UDP-glucuronosyltransferase 1A7 gene and irinotecan toxicity in Japanese cancer patients. *Jpn J Cancer Res* 2002; 93:591–597.
20 Carlini LE, Meropol NJ, Bever J, Andria ML, Hill T, Gold P, et al. UGT1A7 and UGT1A9 polymorphisms predict response and toxicity in colorectal cancer patients treated with capecitabine/irinotecan. *Clin Cancer Res* 2005; 11:1226–1236.
21 Yamanaka H, Nakajima M, Katoh M, Hara Y, Tachibana O, Yamashita J, et al. A novel polymorphism in the promoter region of human UGT1A9 gene (UGT1A9*22) and its effects on the transcriptional activity. *Pharmacogenetics* 2004; 14:329–332.
22 Girard H, Court MH, Bernard O, Fortier LS, Villeneuve L, Hao Q, et al. Identification of common polymorphisms in the promoter of the UGT1A9 gene: evidence that UGT1A9 protein and activity levels are strongly genetically controlled in the liver. *Pharmacogenetics* 2004; 14:501–515.
23 Jinno H, Saeki M, Saito Y, Tanaka-Kagawa T, Hanioka N, Sai K, et al. Functional characterization of human UDP-glucuronosyltransferase 1A9 variant, D256N, found in Japanese cancer patients. *J Pharmacol Exp Ther* 2003; 306:688–693.
24 Jinno H, Saeki M, Tanaka-Kagawa T, Hanioka N, Saito Y, Ozawa S, et al. Functional characterization of wild-type and variant (T202I and M59I) human UDP-glucuronosyltransferase 1A10. *Drug Metab Dispos* 2003; 31:528–532.
25 Kohle C, Mohrle B, Munzel PA, Schwab M, Wernet D, Badary OA, et al. Frequent co-occurrence of the TATA box mutation associated with Gilbert's syndrome (UGT1A1*28) with other polymorphisms of the UDP-glucuronosyltransferase-1 locus (UGT1A6*2 and UGT1A7*3) in Caucasians and Egyptians. *Biochem Pharmacol* 2003; 65:1521–1527.
26 Huang MJ, Yang SS, Lin MS, Huang CS. Polymorphisms of uridine-diphosphoglucuronosyltransferase 1A7 gene in Taiwan Chinese. *World J Gastroenterol* 2005; 11:797–802.
27 Innocenti F, Liu W, Chen P, Dedai AA, Das S, Ratain MJ. Haplotypes of variants in the UDP-glucuronosyltransferase 1A9 and 1A1 genes. *Pharmacogenet Genomics* 2005; 15:295–301.
28 Saeki M, Saito Y, Jinno H, Sai K, Ozawa S, Kurose K, et al. Haplotype structures of the UGT1A gene complex in a Japanese population. *Pharmacogenomics J* 2006; 6:63–75.
29 Sai K, Kaniwa N, Ozawa S, Sawada J. An analytical method for irinotecan (CPT-11) and its metabolites using a high-performance liquid chromatography: parallel detection with fluorescence and mass spectrometry. *Biomed Chromatogr* 2002; 16:209–218.
30 Benjamini Y, Hochberg Y. Controlling the false discovery rate: a practical and powerful approach to multiple testing. *J Rpy Stat Soc B* 1995; 57:289–300.
31 Han JY, Lim HS, Shin ES, Yoo YK, Park YH, Lee JE, et al. Comprehensive analysis of UGT1A polymorphisms predictive for pharmacokinetics and treatment outcome in patients with non-small-cell lung cancer treated with irinotecan and cisplatin. *J Clin Oncol* 2006; 24:2237–2244.
32 Kitagawa C, Ando M, Ando Y, Sekido Y, Wakai K, Imaizumi K, et al. Genetic polymorphism in the phenobarbital-responsive enhancer module of the UDP-glucuronosyltransferase 1A1 gene and irinotecan toxicity. *Pharmacogenet Genomics* 2005; 15:35–41.

CYP2C8 haplotype structures and their influence on pharmacokinetics of paclitaxel in a Japanese population

Yoshiro Saito[a], Noriko Katori[a], Akiko Soyama[a], Yukiko Nakajima[a],
Takashi Yoshitani[a], Su-Ryang Kim[a], Hiromi Fukushima-Uesaka[a],
Kouichi Kurose[a], Nahoko Kaniwa[a], Shogo Ozawa[a], Naoyuki Kamatani[b],
Kazuo Komamura[g,h], Shiro Kamakura[h], Masafumi Kitakaze[h],
Hitonobu Tomoike[h], Kenji Sugai[c], Narihiro Minami[c,d], Hideo Kimura[d],
Yu-ichi Goto[d], Hironobu Minami[i], Teruhiko Yoshida[e], Hideo Kunitoh[f],
Yuichiro Ohe[f], Noboru Yamamoto[f], Tomohide Tamura[f], Nagahiro Saijo[i]
and Jun-ichi Sawada[a]

Objective CYP2C8 is known to metabolize various drugs including an anticancer drug paclitaxel. Although large interindividual differences in CYP2C8 enzymatic activity and several nonsynonymous variations were reported, neither haplotype structures nor their associations with pharmacokinetic parameters of paclitaxel were reported.

Methods Haplotype structures of the CYP2C8 gene were inferred by an expectation-maximization based program using 40 genetic variations detected in 437 Japanese patients, which included cancer patients. Associations of the haplotypes and paclitaxel pharmacokinetic parameters were analyzed for 199 paclitaxel-administered cancer patients.

Results Relatively strong linkage disequilibriums were observed throughout the CYP2C8 gene. We estimated 40 haplotypes without an amino-acid change and nine haplotypes with amino acid changes. The 40 haplotypes were classified into six groups based on network analysis. The patients with heterozygous *IG group haplotypes harboring several intronic variations showed a 2.5-fold higher median area under concentration–time curve of C3'-p-hydroxy-paclitaxel and a 1.6-fold higher median value of C3'-p-hydroxy-paclitaxel/paclitaxel area under concentration–time curve ratio than patients bearing no *IG group haplotypes (P<0.001 for both comparisons by Mann–Whitney U-test). No statistically significant differences, however, were observed between patients with and without the *IG group (haplotypes) in clearance and area under

concentration–time curve of paclitaxel, area under concentration–time curve of 6α-hydroxy-paclitaxel and 6α-, C3'-p-dihydroxy-paclitaxel, and area under concentration–time curve ratio of 6α-hydroxy-paclitaxel/paclitaxel.

Conclusion CYP2C8*IG group haplotypes were associated with increased area under concentration–time curve of C3'-p-hydroxy-paclitaxel and area under concentration–time curve ratio of C3'-p-hydroxy-paclitaxel/paclitaxel. Thus, *IG group haplotypes might be associated with reduced CYP2C8 activity, possibly through its reduced protein levels. Pharmacogenetics and Genomics 17:461–471 © 2007 Lippincott Williams & Wilkins.

Introduction

Cytochrome P450s (CYPs) catalyze oxidative metabolism of a wide variety of exogenous chemicals and endogenous compounds. Human CYP2C subfamily consists of four members, CYP2C18, CYP2C19, CYP2C9, and CYP2C8, all of which are located in tandem on chromosome 10q23–24 in the order listed above [1]. CYP2C8 is a clinically important enzyme, which metabolizes various drugs such as the anticancer drug paclitaxel (PTX), the antiarrhythmic drug amiodarone, the insulin secretagogue repaglinide, the HMG-CoA reductase inhibitor cerivastatin, and the nonsteroidal antiinflammatory drug ibuprofen [1]. This enzyme is also involved in the oxidation of retinoids and fatty acids including arachidonic acid [1].

Up to 38-fold interindividual variability has been reported on PTX 6α-hydroxylation and rosiglitazone p-hydroxylation and N-desmethylation by CYP2C8 [2,3]. Effects of CYP2C8 genetic polymorphisms on metabolic activities have also been studied. Two polymorphisms first identified were 805A > T (Ile269Phe, CYP2C8*2) and 416G > A/1196A > G (Arg139Lys, Lys399Arg, CYP2C8*3). The *2 and *3 alleles were mainly found in Africans with 0.04–0.18 frequencies, and in Caucasians with 0.10–0.23 frequencies, respectively [1]. Both alleles were associated with decreased enzymatic activities for PTX 6α-hydroxylation in vitro [4–6]. CYP2C8*4 allele (792C > G, Ile264Met) was found in British Caucasians [6]. We found 475delA (CYP2C8*5) in Japanese, and this allele leads to a frame shift at codon 159 followed by a stop codon at residue 177 [7]. We also found five additional polymorphisms (CYP2C8*6 to *10) in Japanese [8]. Among them, CYP2C8*7 (556C > T, Arg186X) and *8 (556C > G, Arg186Gly) are different nucleotide variations at the same position. The former variation results in the stop codon, and the latter leads to an amino-acid substitution with a markedly reduced hydroxylation activity to PTX in vitro. Recently, two additional variations, CYP2C8*13 (669T > G, Ile223Met) and *14 (712G > C, Ala238Pro), have been reported [9].

To date, a few reports have shown the impact of CYP2C8*3 alleles on drug pharmacokinetics. The presence of *3 was associated with reduced clearance and increased area under concentration-time curve (AUC) of (R)-ibuprofen [10]. In contrast, significantly reduced AUC and C_{max} of repaglinide were observed in the patients with heterozygous *3 but not in patients with heterozygous *4 [11]. As for PTX, previous studies failed to show the influence of CYP2C8 variations on PTX pharmacokinetics [12,13].

Haplotypes, linked polymorphisms on the same chromosome, often show more precise and strong association with phenotypes such as adverse reaction and/or pharmacokinetics of drugs than individual polymorphisms [14]. In this study, we determined/inferred haplotype structures of the CYP2C8 gene using genetic polymorphisms detected in 437 Japanese patients. Then, association analysis was performed between the haplotypes and pharmacokinetic parameters for PTX and its metabolites. PTX is metabolized to form C3'-p-hydroxy-PTX (3'-p-OH-PTX) and 6α-hydroxy-PTX (6α-OH-PTX): both metabolites are further hydroxylated to 6α-,C3'-p-dihydroxy-PTX (diOH-PTX) [2,15,16]. CYP2C8 metabolizes PTX and 3'-p-OH-PTX into 6α-OH-PTX and diOH-PTX, respectively. Another enzyme, CYP3A4, metabolizes PTX and 6α-OH-PTX into 3'-p-OH-PTX and diOH-PTX, respectively. Previously, we showed that a CYP3A4 haplotype affected the pharmacokinetics of these metabolites [9]. In this study, effects of CYP2C8 haplotypes on PTX metabolism were investigated.

Materials and methods
Patients for DNA sequencing
A total of 437 Japanese patients (235 cancer patients administered PTX, 106 arrhythmic patients, and 96 epileptic patients) participated in this study. This population included 54 patients, who were previously used to identify the CYP2C8*5 allele and four intronic variations [7], and seven patients with CYP2C8*6 to *10 [8], *13 and *14 alleles [9]. Written informed consent was obtained from all participating patients. The ethical review boards of the National Cancer Center, the National Cardiovascular Center, the National Center of Neurology and Psychiatry, and the National Institute of Health Sciences approved this study.

Polymerase chain reaction conditions and DNA sequencing
Genomic DNA was extracted from whole blood leukocytes. First, the entire CYP2C8 gene except for -8.8 and -1.9 kb enhancer regions was amplified in two portions (from the promoter region to exon 5, and exons 6–9) using the primer sets listed in the 'first polymerase chain reaction (PCR)' section of Table 1. Amplification was performed from 200 ng of genomic DNA using 1.25 units of Z-T (Takara Bio. Inc., Shiga, Japan) with 0.2 μmol/l of the primer sets. The first PCR conditions were 30 cycles of 98°C for 5 s, 55°C for 5 s, and 72°C for 190 s. Then, each exon (except for simultaneous amplification of exons 2 and 3) was amplified by Ex-Taq (1.25 units) with a set of primers (0.2 μmol/l) listed in the 'second PCR' section of Table 1 (primers were designed in the intronic regions or promoter region). The second-round PCR conditions were 94°C for 5 min, followed by 30 cycles of 94°C for 30 s, 60°C for 1 min, and 72°C for 2 min, and then a final extension at 72°C for 7 min. As for the -8.8 and -1.9 kb enhancer regions, amplification was performed directly from 50 ng of genomic DNA under the same conditions as in the second round PCR. Thereafter, the PCR products were treated with a PCR Product Pre-Sequencing Kit (USB Co., Cleveland, Ohio, USA) and directly sequenced on both strands using an ABI BigDye Terminator Cycle Sequencing Kit (Applied Biosystems, Foster City, California, USA) with the primers listed in the 'Sequencing' section of Table 1. For the -8.8 and -1.9 kb enhancer regions, promoter region, exon 4, and exons 7–9, the primer sets for the second PCR were also utilized for sequencing. The excess dye was removed by a DyeEx 96 kit (Qiagen, Hilden, Germany). The eluates were applied to an ABI Prism 3700 DNA Analyzer (Applied Biosystems). All detected variations were confirmed by repeating the PCR from the genomic DNA and sequencing of the newly generated PCR products. Genbank accession number NT_030059.12 was used for the reference sequence. Under conditions used, the -8.8 kb enhancer region (pregnanex receptor/constitutive androstane receptor-binding site and its surrounding region), -1.9 kb enhancer region (glucocorticoid receptor-binding site and

Table 1 Primers used for the sequencing of *CYP2C8*

	Amplified and sequenced region	Forward primer Sequences (5'-3')	Position at 5'-end[b]	Reverse primer Sequences (5'-3')	Position at 5'-end[b]	Amplified length (bp)
First PCR	Promoter to exon 5	CTGTGGTGTAAGTGGTAATGAAC	15578696	AAAAGCCCTGAGAACCTATAATC	15563106	15591
	Exons 6-9	TAAGTATTTGTCCCAGTGCTCTC	15562092	TAGCAACTATACAAGCACGGG	15544271	17822
Second PCR	-8.8 kb	CCCAAAAAAGAGCAGGTGTAGCCAT	15586590	TTACTGTCTGTCAAGTGGACCTATC	15586279	312
	-1.9 kb	CTGACCCACATTTTACTCAACTG	15579731	CCCAGTTTAGAGAGGAGAAAGTTAG	15579471	261
	Promoter	GTCCTGTTCTCCCAGAGTTTC	15578600	TCTCCAGAGTGAAAAGAGAAGC	15577623	978
	Exon 1	TCATAAATTCCCAACTGGTC	15578062	GAGCTTGCAGTGAGTGGAGA	15577279	784
	Exons 2-3	TGCTGAATGTGTTGAAGTGAGG	15576234	CTCCCTTGTCTCTGTGCTTC	15575334	901
	Exon 4	AGGCAGTGGATGTGAATAACC	15573481	TCTGTACCTAAAGATTGGAGGCTG	15572897	585
	Exon 5	TCTCAGCATACTATCACAAGGAC	15567211	TAAGGGCTATGTCAATGTGC	15566208	1004
	Exon 6	ACTAACCTAAGCAGCGAATGA	15554467	TTTTCATCTCCCCACCACAGCATT	15553696	772
	Exon 7	GGCTGGTTGTACTTCTGGAC	15551500	AATAGCAGAAAGTCCATCAAGC	15551034	467
	Exon 8	GAAGTGATGAAATAGAGCGGCAA	15547620	TAGTGGCAGAGTTCAGTCAAACC	15546922	699
	Exon 9	TGGGAATAAATAAAGAAATGACTG	15545899	GTCAGCATTAGAAAAGTATTAGCA	15545166	734
Sequencing[a]	Exon 1	CAGTGTTTCTCCATCATCACAGC	15577988	TTCAGAGGGAGTATTTTGCTTT	15577388	
	Exon 2	CATCACAGGCCATCTATAAGTGG	15576165	CCCCCTCACCCCAGTTACC	15575764	
	Exon 3	GGTAACTGGGGTGAGGGGG	15575782	CTCCCTTGTCTCTGTGCTTC	15575334	
	Exon 5	GGAACATTACACACTGGGGT	15567115	ATTATTTTTATTTCAAGAAGAGGG	15566396	
	Exon 6	ACTAACCTAAGCAGCGAATGA	15554467	TCTCTGTCATCCTCCTCCATT	15553904	

[a]Primer sets for the second PCR were used for the -8.8 kb, -1.9 kb, promoter, exons 4, 7, 8 and 9.
[b]The position in the reference sequence, NT_030059.12.

its surrounding region), promoter region (up to 890 bases upstream of the translational initiation site, including hepatocyte nuclear factor 4α-binding site) [17] and all nine exons and its flanking introns were successfully sequenced for all patients analyzed.

Linkage disequilibrium and haplotype analyses

Hardy–Weinberg equilibrium and linkage disequilibrium (LD) analyses were performed by SNPAlyze software (version 3.1, Dynacom Co., Yokohama, Japan), and a pairwise LD between variations was obtained for the $|D'|$ and rho square (r^2) values. Some haplotypes were unambiguously determined from patients with homozygous variations at all sites or a heterozygous variation at only one site. Separately, diplotypes (a combination of haplotypes) were inferred by LDSUPPORT software, which determines the posterior probability distribution of the diplotype configuration for each patient based on estimated haplotype frequencies [18]. Diplotypes of all patients were inferred with probabilities (certainties) of more than 0.95 except for 18 patients. Haplotypes without amino-acid changes were designated as *1, and haplotypes with amino-acid changes were numbered according to the assignments by the Human Cytochrome P450 (CYP) Allele Nomenclature Committee (http://www.cypalleles.ki.se/cyp2c8.htm). The estimated haplotypes (subtypes) were tentatively shown with numbers plus small alphabetical letters. The haplotypes (subtypes) already assigned by the Committee were described as numbers plus capital alphabetical letters (*1A, *1B, and *1C). Network analysis was performed using haplotypes detected in more than two patients with Network 4.1.1.2 by median-joining algorithm (http://fluxus-engineering.com/) [19].

Patients administered PTX and pharmacokinetic analysis

Demographic data of 235 PTX-administered cancer patients including their eligibility criteria were described previously [9]. Of the 235 patients, 199 (185 nonsmall cell lung cancer, four thymic carcinoma, four breast cancer, and six other cancers) were treated with PTX at doses of 175–210 mg/m^2 (the high-dose group in the previous paper [9]) at the National Cancer Center, and used for analysis of associations between haplotypes and pharmacokinetic parameters. These patients consisted of 139 men and 60 women with a mean age of 60.8 (range: 29–81) years. All patients were naive to PTX and pretreated with dexamethasone and an antiallergic agent (diphenhydramine or chlorpheniramine maleate) as prophylactics against hypersensitivity reactions. Carboplatin or nedaplatin was coadministered to almost all patients immediately after PTX treatment. The ethical review boards of both the National Cancer Center and the National Institute of Health Sciences approved this study. Written informed consent was obtained from all patients.

Methods for pharmacokinetic analysis were described previously, and the parameters obtained previously were used for the current association studies [9].

Statistical analysis for association studies

Differences in medians of pharmacokinetic parameters were analyzed by the Kruskal–Wallis test or the Mann–Whitney U-test. Statistical analysis was done using Prism v.4.00 (GraphPad Software Inc., San Diego, California, USA) and SAS v.8.2 (SAS Institute Inc., Cary,

North Carolina, USA). A significance level of 0.05 was applied to all two-tailed analyses.

Results

CYP2C8 variations

We reported previously the *CYP2C8* nonsynonymous variations, *5 (475delA, 159fsX18) [7], *6 (511G > A, Gly171Ser), *7 (556C > T, Arg186X), *8 (556C > G, Arg186Gly,) *9 (740A > G, Lys247Arg), *10 (1149G > T, Lys383Asn) [8], *13 (669T > G, Ile223Met), and *14 (712G > C, Ala238Pro) [9]. These variations were, however, very rare in the Japanese, and it was rather difficult to perform statistical evaluation on their in-vivo associations with altered function, because of low frequencies [9]. Therefore, we continued resequencing this gene including the promoter and intronic regions for up to 437 patients. The enhancer regions were also sequenced for 199 patients administered PTX. Table 2 summarizes the obtained data, where Genbank accession number NT_030059.12 was utilized for the reference sequence. Forty variations, including 11 novel ones, were detected in 437 patients. Because we did not find any significant differences in the genotype distributions among the three disease types ($P \geq 0.05$ by χ^2 test or Fisher's exact test), data from all patients were analyzed as one group. All detected variations were found in Hardy–Weinberg equilibrium ($P \geq 0.05$ by χ^2 test or Fisher's exact test), except for two polymorphisms IVS3–97delT and IVS3–21_–20insT. These deviations were due to the occurrence of one extra homozygote, and the existence of these homozygotes was confirmed by amplification of DNA by another set of primers and resequencing (data not shown). The overall frequencies of the previously reported nonsynonymous variations *CYP2C8*5, *6, *7, *8, *9, *10, *12 (1382_1384del TTG, del 461Val), *13, and *14 were 0.002, 0.002, 0.001, 0.001, 0.001, 0.001, 0.001, 0.001, and 0.001, respectively, and they were all found as heterozygotes. We also detected −271C > A (*CYP2C8*1B*) and −370T > G (*1C*) at frequencies of 0.106 and 0.330, respectively. The frequency of the *1C* allele in Japanese is approximately 5.4-fold higher than in Caucasians [6]. We did not detect any variation in the functional hepatocyte nuclear factor 4α-binding site (−155 to −137 from the translational start site on NT_030059.12) [17], and its surrounding region in 437 patients. Also no variation was found in pregnanex receptor/ constitutive androstane receptor-binding site (−8807 to −8788), glucocorticoid receptor-binding site (−1930 to −1910) [17], and their surrounding regions in 199 PTX-administered patients.

Linkage disequilibrium analysis

Using the 15 detected polymorphisms greater than 0.03 in frequency, LD was analyzed for $|D'|$ and r^2 values (Fig. 1). $|D'|$ values were more than 0.9 in 89 out of 105 (85%) combinations (Fig. 1, lower left). For r^2 values (Fig. 1, upper right), strong LD ($r^2 \geq 0.80$) was observed among IVS2-64A > G, IVS2–13_–12insT, IVS3 −166A > G, IVS4–150G > A, IVS4–94T > C, IVS6 + 196-

G > A, IVS7 + 49T > A, IVS8 + 106G > A, and 1497 (*24)C > T. These polymorphisms were also moderately linked with −411T > C and −370T > G ($r^2 \geq 0.49$). Strong LD was also observed between IVS3-21T > A and IVS4 + 151G > A ($r^2 = 0.93$), and both variations were partially linked with IVS8-204A > G ($r^2 \geq 0.57$). The r^2 values of the other combinations were below 0.33. Collectively, relatively strong LDs were observed throughout the *CYP2C8* gene, suggesting that one LD block covers the entire region analyzed (approximately 33 kb). Thus, *CYP2C8* haplotypes were analyzed as one block.

Haplotype analysis

Haplotypes determined/inferred are shown in Fig. 2. The haplotypes obtained in this study were tentatively shown as a number plus small alphabetical letter except for the haplotypes already publicized on the Human Cytochrome P450 (*CYP*) Allele Nomenclature Committee website, which are described as the number plus capital alphabetical letter (*1A, *1B, and *1C). Several haplotypes were first unambiguously assigned by homozygous single nucleotide polymorphisms at all sites (*1d-*1f, *1j, and *1w) or a heterozygous single nucleotide polymorphism at only one site (*1k, *1m, *1t, *1z, *1aa, and *8b). Separately, diplotypes for each patient were inferred by LDSUPPORT software. The additionally inferred haplotypes were 27 *1 subtypes (*1g, *1h, *1i, *1n to *1s, *1u, *1v, and other very rare 17 haplotypes), and eight haplotypes with nonsynonymous variations (*5b, *6b, *7b, *9b, *10b, *12b, *13b, and *14b). The *1 subtypes inferred in only one patient are grouped into 'others' in Fig. 2, and haplotypes with nonsynonymous variations are described with '?' except for unambiguous *8b, since the predictability for these very rare haplotypes is known to be low in some cases. Overall, 49 haplotypes were determined and/or inferred. The most frequent haplotype was *1d (frequency: 0.366), followed by *1e (0.289), *1f (0.113), and *1B (0.085). Frequencies of the other haplotypes were less than 0.05.

Next, we performed network analysis using haplotypes found in more than two patients to clarify the relationships among the haplotypes. The results showed that the *1 subtypes could be further classified into six groups, *1A, *1B, *1D, *1E, *1G, and *1J groups (Fig. 3). The grouping of *1 subtypes was also shown in Fig. 2. Their frequencies were 0.435 (*1E group), 0.381 (*1D), 0.103 (*1B), 0.030 (*1G), 0.021 (*1A), and 0.013 (*1J). Five rare unclassified *1 subtypes were shown in '*1 others'. Haplotypes *5b and *6b were shown to be derived from *1d and *1B, respectively.

Effects of CYP2C8 haplotypes on PTX metabolism

CYP2C8 catalyzes biotransformation of PTX into 6α-OH-PTX and of 3'-p-OH-PTX into diOH-PTX. The effects of *CYP2C8* haplotypes on PTX clearance, AUCs of PTX

Table 2 Summary of CYP2C8 variations detected in a Japanese population

This study	NCBI (dbSNP)	JSNP	Reference	Location	Position NT_030059.12	From the translational initiation site or from the nearest exon	Nucleotide change and flanking sequences (5' to 3')	Amino acid change	Allele name	Number of subjects Wild-type	Hetero-zygotes	Homo-zygotes	Frequency
MPJ6_2C8029ᵃ	rs7912549		[4]	5'-flanking	15578352_15578350	-667_-665ᵇ	ATAATGTAATAATAA/-CACAAATATTAT			435	2	0	0.002
MPJ6_2C8030	rs17110453		[6]	5'-flanking	15578096	-411ᵇ	ACATTTTTATAT/CACAAAATATAGA			152	218	67	0.403
MPJ6_2C8031	rs7909236		[6]	5'-flanking	15578055	-370ᵇ	CAAGGTCATAAAT/GTCCCAACTGGTC		*1C	201	184	52	0.330
MPJ6_2C8023			[6]	5'-flanking	15577956	-271ᵇ	AGCACATTGGAAC/AAACCAGGGACTT		*1B	352	77	8	0.106
MPJ6_2C8032ᵃ			[7]	Intron 1	15576171	IVS1-197	CTGGGTCATTGCG/ATGGCACATCACA			436	1	0	0.001
MPJ6_2C8014			[4]	Intron 1	15576095	IVS1-121	ATTCAGAAATATC/TGAATCTATGTGT			436	1	0	0.001
MPJ6_2C8010	rs2275622	IMS-JST071855	[4]	Intron 2	15575704	IVS2-64	TGCATGGCTGCCA/GAGTGTTGCAGCA			120	212	105	0.483
MPJ6_2C8001	rs11572078	IMS-JST077576	[7]	Intron 2	15575653_15575652	IVS2-13_-12	AGTTTCTGCCCC-/TTTTTTTATTAG			142	205	90	0.441
MPJ6_2C8015			[7]	Exon 3	15575497	475ᵇ	GAGTTGAGAAAAA/-CCAAGGGTGGGT	159fsX18	*5	435	2	0	0.002
MPJ6_2C8019	rs3752988		[7]	Intron 3	15573409	IVS3-166	AACTCATATTAA/GGGTAAAAGTAAT			141	207	89	0.441
MPJ6_2C8016	rs11572091	IMS-JST105874		Intron 3	15573340	IVS3-97	TTTGTAAGATATT/-GTTAAAAATTTC			427	9	1	0.013
MPJ6_2C8033ᵃ				Intron 3	15573264_15573263	IVS3-21_-20	AATAATTTTTT-/TAAAAATTTTAA			436	0	1	0.002
MPJ6_2C8004	rs7098376		[5]	Intron 3	15573264	IVS3-21	TAATAATTTTTT/AAAAAATTTTAA			409	28	0	0.032
MPJ6_2C8034			[8]	Exon 4	15573214	511ᵇ	ACTTTCATCCTGG/AGCGTGTCTCCCT	Gly171Ser	*6	435	2	0	0.002
MPJ6_2C8035			[8]	Exon 4	15573169	556ᵇ	GTTTTCCAGAAAC/TGATTTGATTATA	Arg186X	*7	436	1	0	0.001
MPJ6_2C8036			[8]	Exon 4	15573169	556ᵇ	GTTTTCCAGAAAC/GGATTTGATTATA	Arg186Gly	*8	436	1	0	0.001
MPJ6_2C8037ᵃ			[4]	Intron 4	15573039	IVS4+44	CATTATTCAAGG/TTTGTAGGGAAGA			436	1	0	0.001
MPJ6_2C8024	rs11572093			Intron 4	15572932	IVS4+151	CTTTGATTCCTG/ATTCAAAATTTC			411	26	0	0.030
MPJ6_2C8038ᵃ				Intron 4	15567024	IVS4-230	GACGAGTTATGG/AGTGCAGTGACACC			436	1	0	0.001
MPJ6_2C8039ᵃ				Intron 4	15567008	IVS4-214	CAGTACACCAACC/ATGGCACATGTAT			436	1	0	0.001
MPJ6_2C8020	rs1926705			Intron 4	15566944	IVS4-150	AGAACTAAAGTG/ATAATAAAAATG			119	214	104	0.483
MPJ6_2C8025ᵃ				Intron 4	15566937	IVS4-143	AAAGTGTAATAAA/GAAATGTATATAT			436	1	0	0.001
MPJ6_2C8012	rs11572101			Intron 4	15566888	IVS4-94	GACATGATGTCTT/CATTCATATTTAT			141	207	89	0.441
MPJ6_2C8040			[9]	Exon 5	15566768	669ᵇ	CCCTCTACTCATT/GGATTGTTTCCCA	Ile223Met	*13	436	1	0	0.001
MPJ6_2C8041			[9]	Exon 5	15566725	712ᵇ	CTTAAAAATGTTG/CCTCTTACACGAA	Ala238Pro	*14	436	1	0	0.001
MPJ6_2C8026			[8]	Exon 5	15566697	740ᵇ	ACATTAGGGAGAA/GAGTAAAAGAAACA	Lys247Arg	*9	436	1	0	0.001
MPJ6_2C8027ᵃ				Intron 5	15566597	IVS5+21	TTAGCAACAGATC/TAGTATTTGATT			435	2	0	0.002
MPJ6_2C8042ᵃ				Intron 6	15553909	IVS6+184	GGAGGAGGATGAC/GAGAGATCAGTAG			433	4	0	0.005
MPJ6_2C8021	rs1891071	IMS-JST082397		Intron 6	15553897	IVS6+196	CAGAGATCAGTAG/AAAACAGTATGGC			124	215	98	0.470
MPJ6_2C8043ᵃ				Intron 6	15553794	IVS6+299	ATTGCCCTAGTAT/CTGAATGTTGGTT			436	1	0	0.001
MPJ6_2C8044			[8]	Exon 7	15551173	1149ᵇ	CCTCATCCCCAAG/TGTAAGCTTGTTT	Lys383Asn	*10	436	1	0	0.001
MPJ6_2C8013	rs2275620	IMS-JST071852	[4]	Intron 7	15551124	IVS7+49	CTGAAATTCCAT/AAGTGCTGGTTG			124	215	98	0.470
MPJ6_2C8017			[7]	Intron 7	15551102	IVS7+71	TTGGTTCCAACCC/TTCTAACACACA			430	7	0	0.008
MPJ6_2C8007			[5]	Exon 8	15547241	1230ᵇ	CTTTGACCCTGGC/TCACTTCTCTAGAT	Gly410Gly		424	13	0	0.015
MPJ6_2C8008	rs1934951	IMS-JST071853	[5]	Intron 8	15547074	IVS8+106	GAATTGCTATTTG/ATCCATGATCAAG			143	201	93	0.443
MPJ6_2C8022	rs2275621	IMS-JST071854		Intron 8	15547050	IVS8+130	GAGCACCCACTCTT/CAACACCCATGTG			430	7	0	0.008
MPJ6_2C8018	rs11572177		[7]	Intron 8	15545796	IVS8-204	GATAGCAAATATA/GTCTCTTTTGTA			403	33	1	0.040
MPJ6_2C8045	rs3832694	IMS-JST091412	[5]	Exon 9	15545502_15545500	1382_1384ᵇ	ACCTGAAATCTGTTG/-ATGATTTAAAGA	del 461Val	*12	436	1	0	0.001
MPJ6_2C8009	rs1058932	IMS-JST091413		3'-UTR	15545387	1497ᵇ(*24)ᶜ	CCATCTGGCTGCC/TGATCTGCTATCA			143	196	98	0.449
MPJ6_2C8046ᵃ				3'-UTR	15545208	1676ᵇ(*203)ᶜ	ACTCTGTAACACT/-TGTATTAATTGC			434	3	0	0.003

ᵃNovel variations detected in our study.
ᵇA of the translation initiation codon ATG is numbered +1.
ᶜThe nucleotide number from the end of translational termination codon.
SNP, single nucleotide polymorphism.

Fig. 1
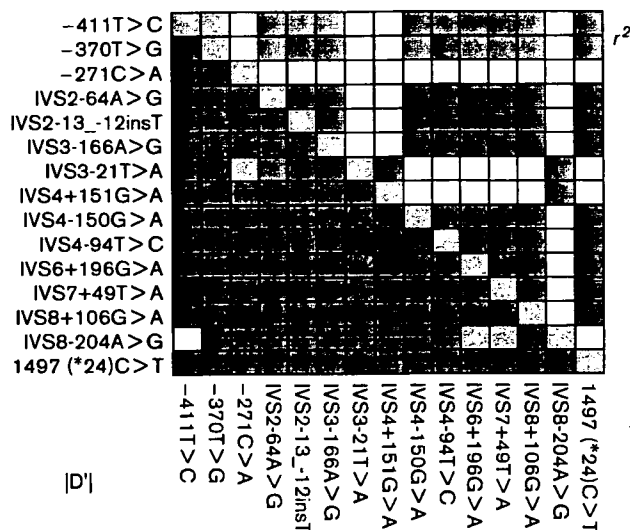
Linkage disequilibrium (LD) analysis of CYP2C8. Pairwise LD between variations with ≥ 3% frequencies is expressed as |D'| (lower left) and r^2 (upper right) by 10-graded blue colors. A denser color represents a higher linkage.

and its metabolites, and metabolic ratios (ratios of metabolite AUCs to PTX AUC) were investigated in 199 PTX-administered patients.

Because nonsynonymous variations were all rare, we focused on the effects of diplotypes using grouped *1 haplotypes (i.e. *1A, *1B, etc). No significant differences were observed in clearance of PTX, AUCs of PTX, 6α-OH-PTX and diOH-PTX, and AUC ratio of 6α-OH-PTX/ PTX among the grouped *1-diplotypes found in more than three patients (data not shown). A statistically significant deviation, however, was observed in AUC of 3'-p-OH-PTX among the grouped *1-diplotypes ($n \geq 3$) ($P = 0.014$ by Kruskal–Wallis test) (Fig. 4a). Furthermore, AUC ratio of 3'-p-OH-PTX/PTX also showed a tendency to be different among the grouped *1-diplotypes of $n \geq 3$ by the same test ($P = 0.071$) (Fig. 4b). Careful analysis revealed that significant differences in both parameters were observed between *1D/*1D and *1G/*1D patients ($P < 0.05$ for both parameters, Mann–Whitney U-test) and between *1E/*1E and *1G/*1E patients ($P < 0.001$ for AUC of 3'-p-OH-PTX and $P < 0.01$ for AUC ratio of 3'-p-OH-PTX/PTX) (Fig. 4).

Next, heterozygous *1G diplotypes were combined into *1G/non-*1G diplotypes ($n = 11$). Because no significant differences were observed among the other *1/*1 groups, all the other *1/*1 diplotypes were combined into one group, designated as non-*1G/non-*1G. As shown in Fig. 5a, the median AUC of 3'-p-OH-PTX was about 2.5-fold

higher in the *1G/non-*1G patients than in the non-*1G/ non-*1G patients ($P < 0.001$ by Mann–Whitney U-test). The median value of 3'-p-OH-PTX/PTX AUC ratio was also about 64% higher in the *1G/non-*1G patients than in the non-*1G/non-*1G patients ($P < 0.001$, Fig. 5b). In contrast, there were no significant differences in AUC of 6α-OH-PTX and AUC ratio of 6α-OH-PTX/PTX between the two groups (Fig. 5c and d) although the AUC ratio was about 9% lower in the *1G/non-*1G patients than in the non-*1G/non-*1G patients (Fig. 5d). Considering the metabolic route of PTX, these findings suggest that CYP2C8 activity is probably reduced in the *1G-bearing patients.
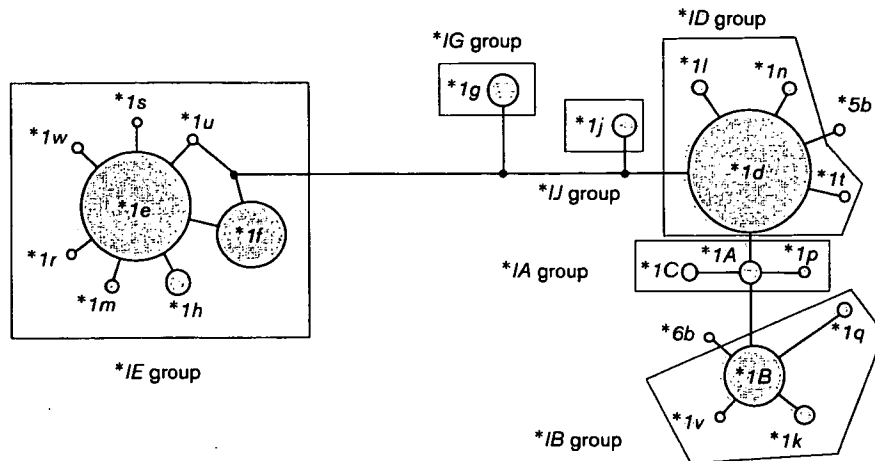
Recently, we have shown that CYP3A4*16B (and probably *6, $n = 1$) decreases the AUC ratio of 3'-p-OH-PTX/PTX, and that no other major CYP3A4 haplotypes significantly affect the AUC ratio and other PK parameters analyzed [9]. Therefore, we analyzed the effects of *1G on the AUC of 3'-p-OH-PTX and AUC ratio of 3'-p-OH-PTX/ PTX excluding CYP3A4*16B- and *6-bearing patients and confirmed the increasing effects of *1G ($P < 0.001$ for both by Mann–Whitney U-test). In addition, the significantly increasing effects of CYP2C8*1G were also observed within CYP3A4*1A/*1A patients ($P < 0.001$ for AUC of 3'-p-OH-PTX and $P < 0.01$ for AUC ratio of 3'-p-OH-PTX/PTX, Mann–Whitney U-test). Furthermore, distributions of CYP3A4 diplotypes/haplotypes were not significantly different between the CYP2C8*1G/non-*1G patients and the non-*1G/non-*1G patients ($P > 0.05$ by Fisher's exact test). These results suggest that the effects of CYP2C8*1G are independent of the CYP3A4 genotypes. Gender also affects the AUC ratio of 3'-p-OH-PTX/PTX [9]. Statistical analysis using data from men only also gave almost the same increasing effects of *1G ($P < 0.001$ for the AUC of 3'-p-OH-PTX and $P = 0.001$ for the AUC ratio of 3'-p-OH-PTX/PTX, Mann–Whitney U-test).

To identify further the genetic variation responsible for the increased AUC of 3'-p-OH-PTX and increased AUC ratio of 3'-p-OH-PTX/PTX, we next focused on the variations in the *1G group. Among them, the patients bearing IVS3-21T > A showed statistically significant increases in these parameters compared with the patients without this variation ($P < 0.001$ for both parameters, Mann–Whitney U-test). The *1t haplotype also harbored IVS3-21T > A, and one patient with the *1t/*1d diplotype (grouped into *1D/*1D) had the second highest AUC of 3'-p-OH-PTX (1.07 h*μg/ml) and the second highest AUC ratio of 3'-p-OH-PTX/PTX (0.0497) in the 24 *1D/*1D patients (Fig. 4, grey arrowheads). These findings suggest that IVS3-21T > A might be involved in the altered CYP2C8 activity, although we cannot exclude the possibility that other identified/unidentified linked variation is causative.

Fig. 2

Haplotype structures of *CYP2C8* in Japanese population. Haplotypes are described with numbers plus alphabetical letters, and the *1 haplotypes (without amino-acid change) were grouped based on network analysis (Fig. 3). Because rare *1 haplotypes found in only one individual were grouped into 'others', the seven variations detected only in the rare haplotypes (IVS1 – 197G>A, IVS1 −121C>T, IVS4 + 44G>T, IVS4 −230G>A, IVS4 −214C>A, IVS4 −143A>G, and IVS6 + 299T>C) are not shown in this figure. Numbers in parenthesis in the 'Number' section indicate patient numbers used for association analysis for pharmacokinetic parameters of PTX. White, major allele; yellow with a haplotype name, minor allele; yellow without a haplotype name in 'others', common variations of the 'others' group. In yellow with a haplotype name, nonsynonymous variations are shown by a red number.

Fig. 3

Network analysis of CYP2C8 haplotypes. Haplotypes found in at least two patients are shown. The areas of each circle represent the approximate frequency of each haplotype. The *1 subgroups are enclosed by red lines.

Discussion

All nonsynonymous variations of CYP2C8 found in Japanese were rare (frequencies ≤ 0.002), and thus we could not apply statistical analysis for their associations with pharmacokinetic parameters of PTX [9]. As shown in Fig. 4b, the AUC ratio of 3'-p-OH-PTX/PTX of a patient with heterozygous *5b haplotype (with 475delA, 159fsX18, no activity) was, however, the third highest (2.8-fold higher than median value) in all 199 patients analyzed. In addition, the patient with heterozygous *7b (with 556C > T, Arg186X, no activity) had the lowest AUC ratio of 6α-OH-PTX/PTX (approximately one-fifth of the median value) (data not shown). Thus, at least some of the nonsynonymous CYP2C8 variations described in this paper probably affect the PTX metabolism in vivo. These rare variations, however, cannot fully explain the interindividual differences in the CYP2C8 activity. Therefore, we focused on the *1 haplotypes without amino-acid change. The estimated CYP2C8 *1 haplotypes could be classified into six haplotype groups (*1A, *1B, *1D, *1E, *1G, and *1J) based on network analysis, and their effects on PTX metabolism were analyzed.

This study revealed that the AUC of 3'-p-OH-PTX and AUC ratio of 3'-p-OH-PTX/PTX were increased in the *1G-bearing patients. It must be noted that AUC of 3'-p-OH-PTX was considerably increased (2.5-fold). The 3'-p-OH-PTX is generated from PTX by CYP3A4 and metabolized into diOH-PTX by CYP2C8. Thus, both CYP2C8 and CYP3A4 activities can influence the AUC of 3'-p-OH-PTX. In the previous study [9], we have shown that the CYP3A4*16B haplotype harboring 554C > G (Thr185Ser), but not the other haplotypes, increases the AUC ratio of 6α-OH-PTX/PTX and decreases the

AUC ratio of 3'-p-OH-PTX/PTX with statistical significance. In addition, gender difference was also shown to affect both AUC ratios [9].The association of CYP2C8*1G group haplotypes with increased AUC of 3'-p-OH-PTX and AUC ratio of 3'-p-OH-PTX/PTX, however, could not be explained by the influence of CYP3A4*16B (and theoretically null haplotype *6) or gender difference since the same conclusions were obtained even if patients with CYP3A4*16B and *6, or females were excluded. Moreover, statistical analysis using data only from CYP3A4*1A/*1A patients also gave almost the same effects of *1G on the AUC of 3'-p-OH-PTX and the AUC ratio of 3'-p-OH-PTX/PTX, suggesting that the effects of CYP2C8*1G are independent of the CYP3A4 genotypes or gender difference. Thus, the increased AUC of 3'-p-OH-PTX and AUC ratio of 3'-p-OH-PTX/PTX can be attributed to CYP2C8*1G, suggesting reduced CYP2C8 activity in patients with *1G. Moreover, transporters such as P-glycoprotein encoded by the ABCB1 gene could contribute to the AUCs of PTX and its metabolites [20]. We reported previously that AUC of 3'-p-OH-PTX was slightly increased in the patients bearing *2 haplotype in block 2 of ABCB1 (1236C > T, 2677G > T, and 3435C > T) [9]. When the frequencies of the *2 haplotype were compared between the CYP2C8*1G/non-*1G patients and the non-*1G/non-*1G patients, however, no statistically significant difference was observed (P = 0.705 by χ^2 test).

CYP2C8*1G group haplotypes harbors several variations, which are all located in introns. Thus, the mechanism for the increased AUC of 3'-p-OH-PTX and AUC ratio of 3'-p-OH-PTX/PTX is not caused by an amino-acid change. Among the variations in the *1G group, IVS3–21T > A

Fig. 4
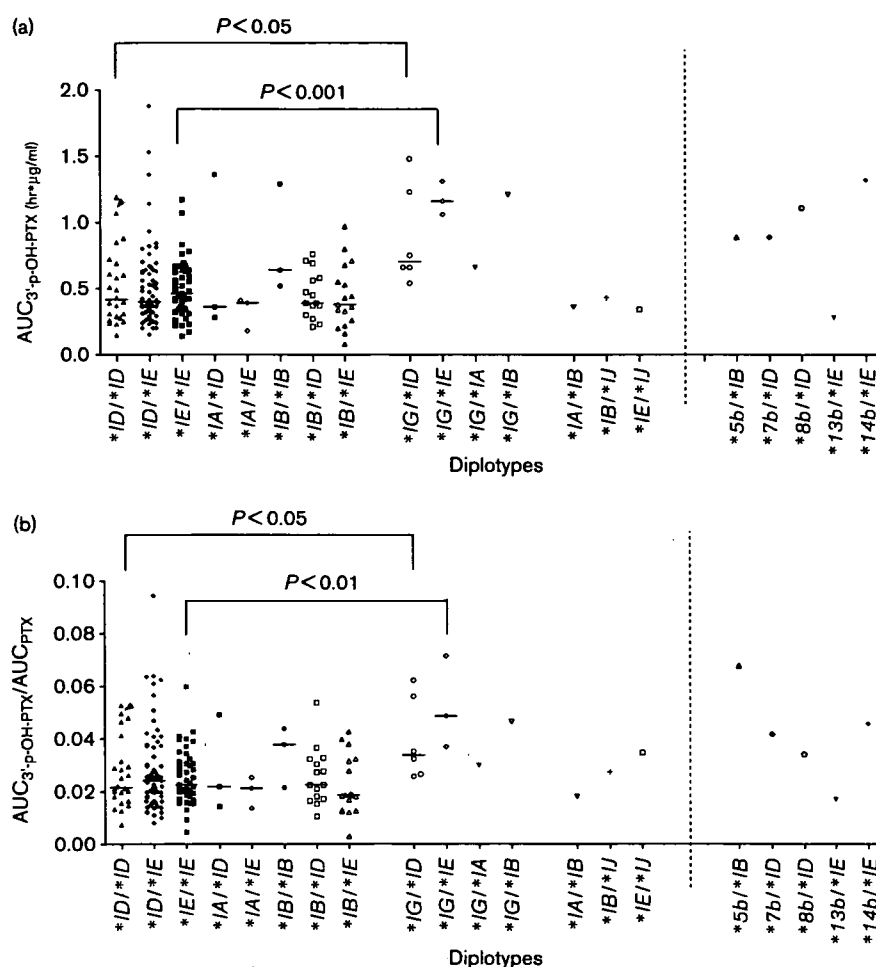
Effects of CYP2C8 diplotypes on AUC of 3'-p-OH-PTX (a), and AUC ratio of 3'-p-OH-PTX/PTX (b). All combinations of diplotypes using grouped haplotypes for *1 are shown. Grey arrowheads indicate patients with heterozygous *1t haplotype. Statistical significance was analyzed by the Mann–Whitney U-test to reveal the effects of *IG group haplotypes. AUC, area under concentration–time curve; PTX, paclitaxel.

and IVS4 + 151G > A were relatively *IG group specific. Because the patient with *1t haplotype also had a high AUC of 3'-p-OH-PTX and a high AUC ratio of 3'-p-OH-PTX/PTX, it is possible that the IVS3 – 21T > A could be a functionally causing variation rather than IVS4 + 151G > A. Because IVS3-21T > A is located in the T-rich (pyrimidine-rich) region upstream of a splice acceptor site and this polypyrimidine tract is important for efficient RNA spliceosome assembly [21], this transversion could reduce the expression level of mature CYP2C8 mRNA, resulting in reduced protein expression levels. We cannot, however, exclude the possibility that other identified/unidentified linked variation could be causative.

We did not observe significant differences in the AUC of 6α-OH-PTX and AUC ratio of 6α-OH-PTX/PTX between the heterozygous *IG patients and non-*IG/non-*IG patients. This is surprising because CYP2C8 is

considered to be the major enzyme responsible for 6α-hydroxylation of PTX. Currently, we have no data for explaining this. It is noteworthy that the CYP3A4*16B haplotype more clearly affects the increase in AUC ratio of 6α-OH-PTX/PTX than the decrease in AUC ratio of 3'-p-OH-PTX/PTX [9]. CYP3A4- and CYP2C8-mediated disappearance processes of 6α-OH-PTX and 3'-p-OH-PTX, respectively, might be more influential to their AUCs than their generation from PTX. One alternative (less likely) possibility is that another unidentified enzyme also catalyzes the transformation of PTX into 6α-OH-PTX in vivo, and that the effect of reduced CYP2C8 activity is not clearly reflected in the parameters analyzed.

Neither the normalized clearance nor AUC of PTX was significantly influenced by CYP2C8 diplotypes. The small effect of *IG on PTX clearance may be partly explained

Fig. 5
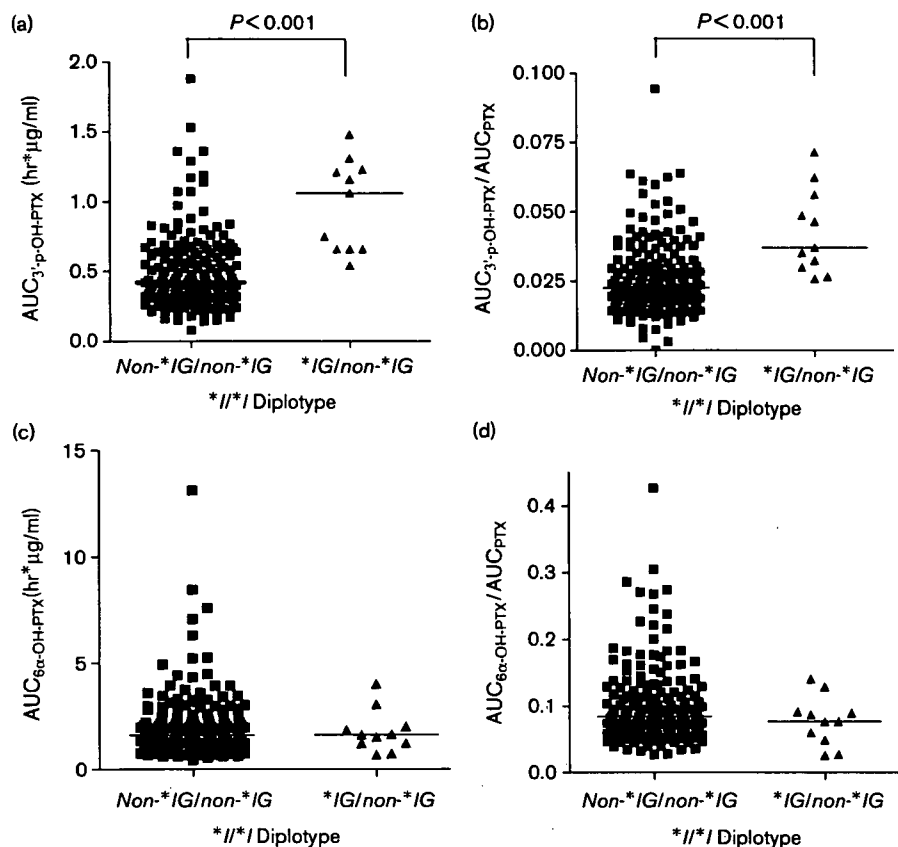
Effects of CYP2C8*IG group haplotypes on AUC of 3'-p-OH-PTX (a), AUC ratio of 3'-p-OH-PTX/PTX (b), AUC of 6α-OH-PTX (c), and AUC ratio of 6α-OH-PTX/PTX (d). Statistical significance was analyzed by the Mann–Whitney U-test. AUC, area under concentration–time curve; PTX, paclitaxel.

by only small fraction of PTX to be metabolized. In fact, median AUC of 3'-p-OH-PTX (0.50 h/mol/l) and 6α-OH-PTX (1.85 h/mol/l) was only 2.3 and 8.5% of that of AUC of PTX (21.67 h/mol/l), respectively.

Recently, Nakajima et al. [13] tried to analyze the effects of CYP2C8 polymorphisms on PTX pharmacokinetics. They genotyped 11 nonsynonymous variations including CYP2C8*5, but none were detected from 23 Japanese ovarian cancer patients. Also, we could not apply statistical analysis to the pharmacokinetic parameters for five nonsynonymous variations as described above since the nonsynonymous variations are all rare in Japanese. Rather, *IG group haplotypes (and possibly *It) are probably important for PTX metabolism. The effect of this group haplotypes tagged by IVS3–21T > A on pharmacokinetics of other CYP2C8-catalyzing drugs must be clarified in the future.

In conclusion, we determined/inferred a total of 49 haplotypes using the detected variations in the CYP2C8 gene from 437 Japanese patients. CYP2C8*IG group

haplotypes, consisting of intronic variations, were found to be associated with significantly increased AUC of the PTX metabolite 3'-p-OH-PTX and the AUC ratio of 3'-p-OH-PTX/PTX. Thus, CYP2C8*IG group haplotypes may influence CYP2C8 activity, although the causative variation is not fully identified.

Acknowledgements

References

1 Totah RA, Rettie AE. Cytochrome P450 2C8: substrates, inhibitors, pharmacogenetics, and clinical relevance. Clin Pharmacol Ther 2005; 77:341–352.

2   Sonnichsen DS, Liu Q, Schuetz EG, Schuetz JD, Pappo A, Relling MV. Variability in human cytochrome P450 paclitaxel metabolism. *J Pharmacol Exp Ther* 1995; **275**:566–575.

3   Baldwin SJ, Clarke SE, Chenery RJ. Characterization of the cytochrome P450 enzymes involved in the in vitro metabolism of rosiglitazone. *Br J Clin Pharmacol* 1999; **48**:424–432.

4   Dai D, Zeldin DC, Blaisdell JA, Chanas B, Coulter SJ, Ghanayem BI, *et al.* Polymorphisms in human CYP2C8 decrease metabolism of the anticancer drug paclitaxel and arachidonic acid. *Pharmacogenetics* 2001; **11**:597–607.

5   Soyama A, Saito Y, Hanioka N, Murayama N, Nakajima O, Katori N, *et al.* Non-synonymous single nucleotide alterations found in the CYP2C8 gene result in reduced in vitro paclitaxel metabolism. *Biol Pharm Bull* 2001; **24**:1427–1430.

6   Bahadur N, Leathart JB, Mutch E, Steimel-Crespi D, Dunn SA, Gilissen R, *et al.* CYP2C8 polymorphisms in Caucasians and their relationship with paclitaxel 6alpha-hydroxylase activity in human liver microsomes. *Biochem Pharmacol* 2002; **64**:1579–1589.

7   Soyama A, Saito Y, Komamura K, Ueno K, Kamakura S, Ozawa S, *et al.* Five novel single nucleotide polymorphisms in the CYP2C8 gene, one of which induces a frame-shift. *Drug Metab Pharmacokinet* 2002; **17**:374–377.

8   Hichiya H, Tanaka-Kagawa T, Soyama A, Jinno H, Koyano S, Katori N, *et al.* Functional characterization of five novel CYP2C8 variants, G171S, R186X, R186G, K247R, and K383N, found in a Japanese population. *Drug Metab Dispos* 2005; **33**:630–636.

9   Nakajima Y, Yoshitani T, Fukushima-Uesaka H, Saito Y, Kaniwa N, Kurose K, *et al.* Impact of the haplotype CYP3A4*16B harboring the Thr185Ser substitution on paclitaxel metabolism in Japanese cancer patients. *Clin Pharmacol Ther* 2006; **80**:179–191.

10 Martinez C, Garcia-Martin E, Blanco G, Gamito FJ, Ladero JM, Agundez JA. The effect of the cytochrome P450 CYP2C8 polymorphism on the disposition of (R)-ibuprofen enantiomer in healthy subjects. *Br J Clin Pharmacol* 2005; **59**:62–68.

11 Niemi M, Leathart JB, Neuvonen M, Backman JT, Daly AK, Neuvonen PJ. Polymorphism in CYP2C8 is associated with reduced plasma concentrations of repaglinide. *Clin Pharmacol Ther* 2003; **74**:380–387.

12 Henningsson A, Marsh S, Loos WJ, Karlsson MO, Garsa A, Mross K, *et al.* Association of CYP2C8, CYP3A4, CYP3A5, and ABCB1 polymorphisms with the pharmacokinetics of paclitaxel. *Clin Cancer Res* 2005; **11**: 8097–8104.

13 Nakajima M, Fujiki Y, Noda K, Ohtsuka H, Ohkuni H, Kyo S, *et al.* Pharmacokinetics of paclitaxel in ovarian cancer patients and genetic polymorphisms of CYP2C8, CYP3A4, and MDR1. *J Clin Pharmacol* 2005; **45**:674–682.

14 Judson R, Stephens JC, Windemuth A. The predictive power of haplotypes in clinical response. *Pharmacogenomics* 2000; **1**:15–26.

15 Monsarrat B, Chatelut E, Royer I, Alvinerie P, Dubois J, Dezeuse A, *et al.* Modification of paclitaxel metabolism in a cancer patient by induction of cytochrome P450 3A4. *Drug Metab Dispos* 1998; **26**:229–233.

16 Taniguchi R, Kumai T, Matsumoto N, Watanabe M, Kamio K, Suzuki S, *et al.* Utilization of human liver microsomes to explain individual differences in paclitaxel metabolism by CYP2C8 and CYP3A4. *J Pharmacol Sci* 2005; **97**:83–90.

17 Ferguson SS, Chen Y, LeCluyse EL, Negishi M, Goldstein JA. Human CYP2C8 is transcriptionally regulated by the nuclear receptors constitutive androstane receptor, pregnanex receptor, glucocorticoid receptor, and hepatic nuclear factor 4α. *Mol Pharmacol* 2005; **68**:747–757.

18 Kitamura Y, Moriguchi M, Kaneko H, Morisaki H, Morisaki T, Toyama K, *et al.* Determination of probability distribution of diplotype configuration (diplotype distribution) for each subject from genotypic data using the EM algorithm. *Ann Hum Genet* 2002; **66**:183–193.

19 Bandelt HJ, Forster P, Rohl A. Median-joining networks for inferring intraspecific phylogenies. *Mol Biol Evol* 1999; **16**:37–48.

20 Lehnert M, Emerson S, Dalton WS, de Giuli R, Salmon SE. In vitro evaluation of chemosensitizers for clinical reversal of P-glycoprotein-associated Taxol resistance. *J Natl Cancer Inst Monogr* 1993; **15**:63–67.

21 Roscigno RF, Weiner M, Garcia-Blanco MA. A mutational analysis of the polypyrimidine tract of introns. Effects of sequence differences in pyrimidine tracts on splicing. *J Biol Chem* 1993; **268**:11222–11229.